Supporting Information

Tungstosulfonic acid as an efficient solid acid catalyst for acylal synthesis for the protection of aldehydic carbonyl group

Reddi Mohan Naidu Kalla, Mi Ri Kim, Yu Na Kim, Il Kim *

BK21 PLUS Center for Advanced Chemical Technology, Department of Polymer Science and Engineering, Pusan National University, Busan 609-735, Republic of Korea

Table of contents

1. Synthesis of TSA.

A 50-mL reaction flask was equipped with a constant-pressure dropping funnel. The gas outlet was connected to a vacuum system through an alkali solution trap. Tungstic acid (TA) (1 mmol) was added to the flask, and chlorosulfonic acid (2 mmol) in CH_2Cl_2 (10 mL) was added drop-wise over a period of 15 min at room temperature. After the addition, the mixture was stirred for 2 h, and the residual HCl was eliminated by suction. The mixture was then washed with CH_2Cl_2, and the TSA product was obtained as a greenish solid (Scheme S1).

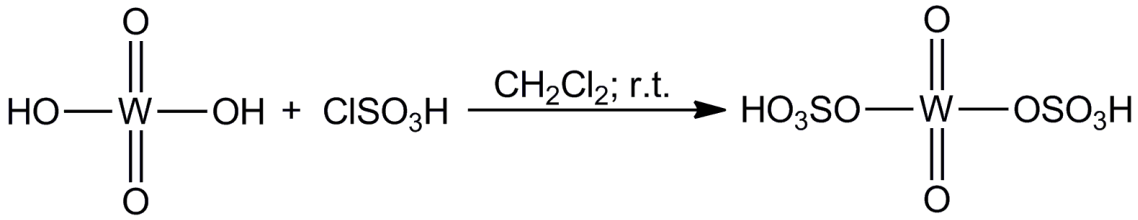

Scheme S1. Preparation of the solid acid TSA.

2. Characterization of TSA

The FT-IR spectra of TA and TSA are depicted in Fig. S1. The spectrum of TA shows an OH stretching frequency at 3402 cm^{-1}, while that of TSA shows the O–H stretch of the SO_3H group at 3385 cm^{-1}.The bands at 1280 and 1179 cm^{-1}, which correspond, to the asymmetric and symmetric O=S=O stretching peaks respectively, and the S–O stretching peak at 851 cm^{-1} confirm the presence of the SO_3 group. The observed sulfonation peaks are in good agreement with previously reported one[3]. In addition, the absence of peaks at 1280 and 1179 cm^{-1} in the spectrum of TA indicates that sulfonation has occurred to produce TSA.

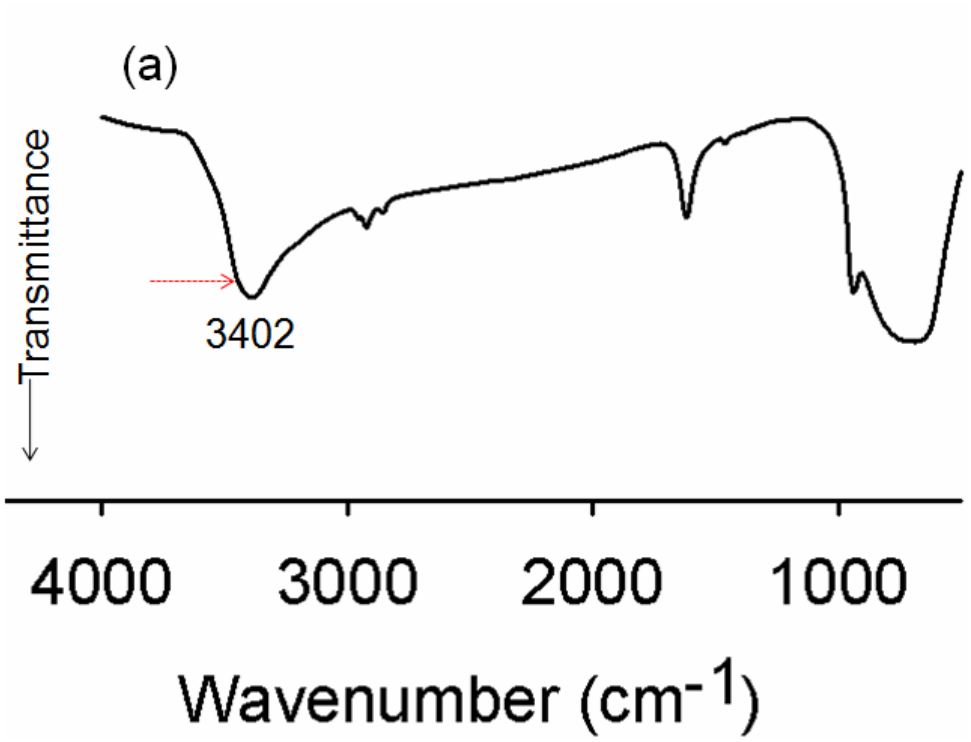

Fig. S1 (a). FT-IR spectra of TA.

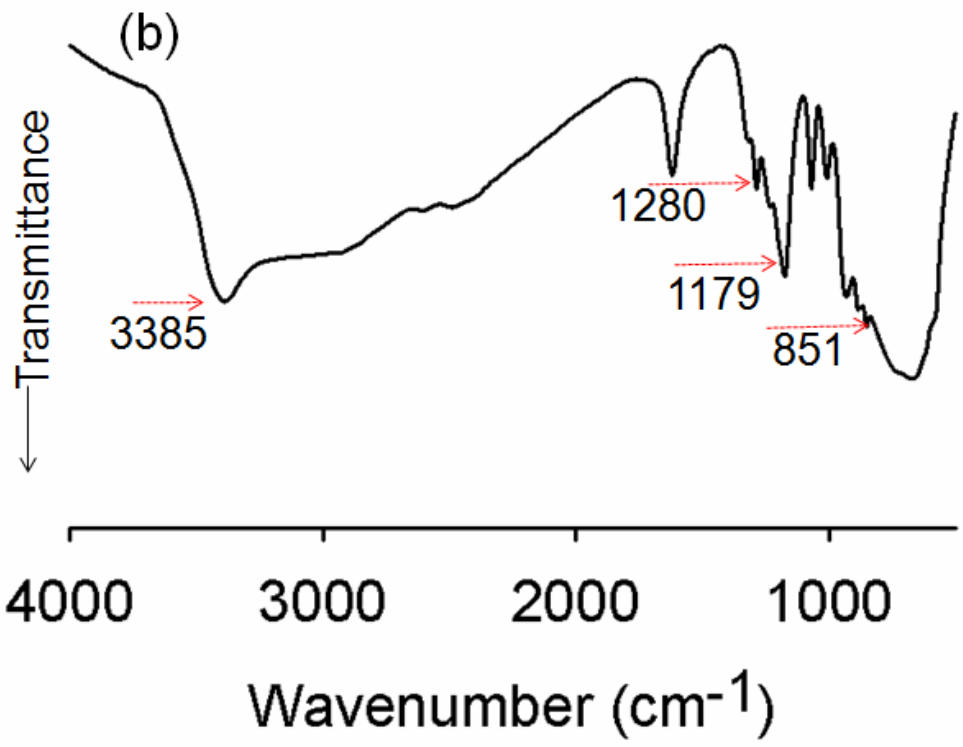

Fig. S1 (b). FT-IR spectra of TSA.

The sulfonation of TA was further confirmed by X-ray powder diffraction (XRD) analysis (Fig. S2). The XRD analysis shows that the diffraction pattern of the TA (Figure 2a) differs from that of TSA (Figure 2b) as a result of sulfonation. The peak intensities, particularly at 2θ=25–30°, are reduced following sulfonation consistent with introduction of the SO_3 group as well as the orientation of the crystal structure. SEM analysis was employed to study the surface morphology of TA and TSA (Fig. S3a and b). The SEM image of TA shows the presence of well dispersed particles of uniform size and shape. On the other hand, the SEM image of TSA shows particles with different surface morphology due to the incorporation of $–SO_3H$ in TA. The increased reactivity of sulfonic-acid-functionalised on TA is believed to be due to sulfonic-acid-support interactions and the resulting changes in surface properties of the reactive sites. Sulfonation also was confirmed by energy dispersive X-ray (EDX) analysis (inset in Fig. 3a and b), which shows the presence of W, O and S in TSA, whereas a signal for sulfur is absent in TA.

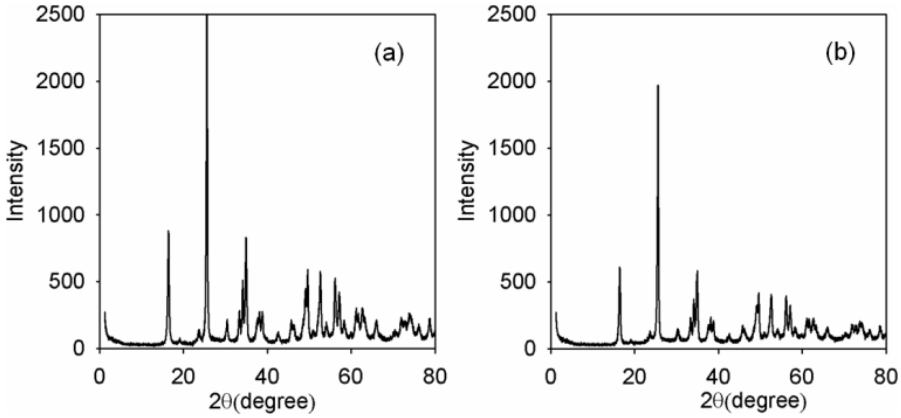

Fig. S2. XRD patterns of (a) TA and (b) TSA.

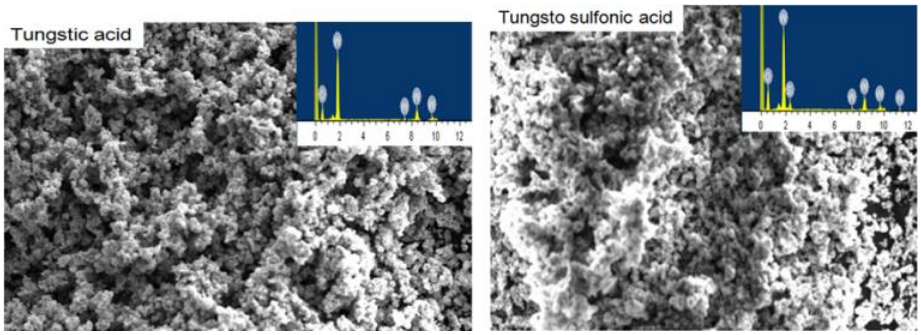

Fig. S3. SEM images of (a) TA and (b) TSA. Insets are an EDX spectrum of each sample.

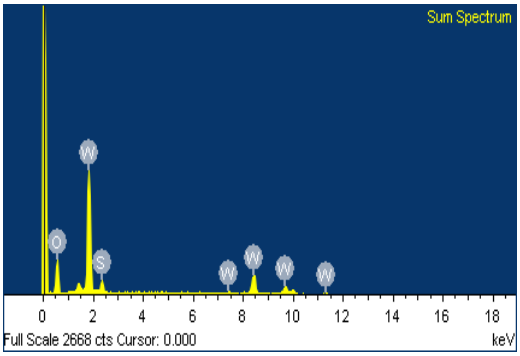

Fig. S4. EDX spectrum of TSA.

3. Preparation of acylals (1-25).

In a 50-mL round bottom flask TSA (2.5 mol %) was added to a mixture of p-methyl benzaldehyde (1 mmol) and acetic anhydride (1 mmol). The reaction mixture was stirred at room temperature becoming solid within 2 min. Chloroform was added, and the insoluble catalyst was separated by simple filtration, washed twice with chloroform, and dried at 100 ℃ for 2h for reuse. The chloroform filtrate was evaporated under reduced pressure, and the solid obtained was washed with petroleum ether (20 mL) for three times and recrystallization form dichloromethane to afford the resulting acylal, **1**.

4. IR, ^{1}H and $^{13}CNMR$ spectra for the selected acylals

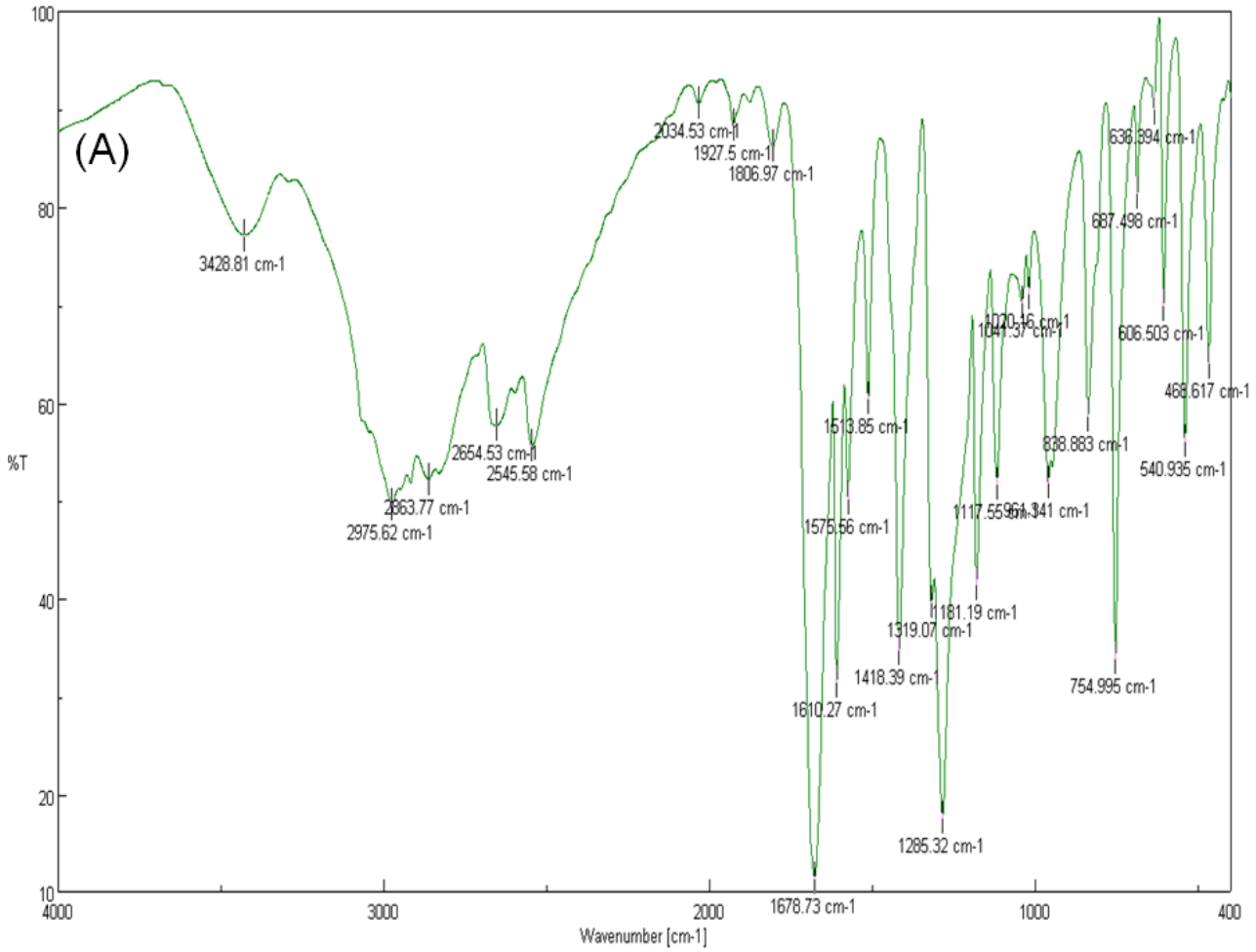

Fig. S5 (A) IR spectra of entry **1**.

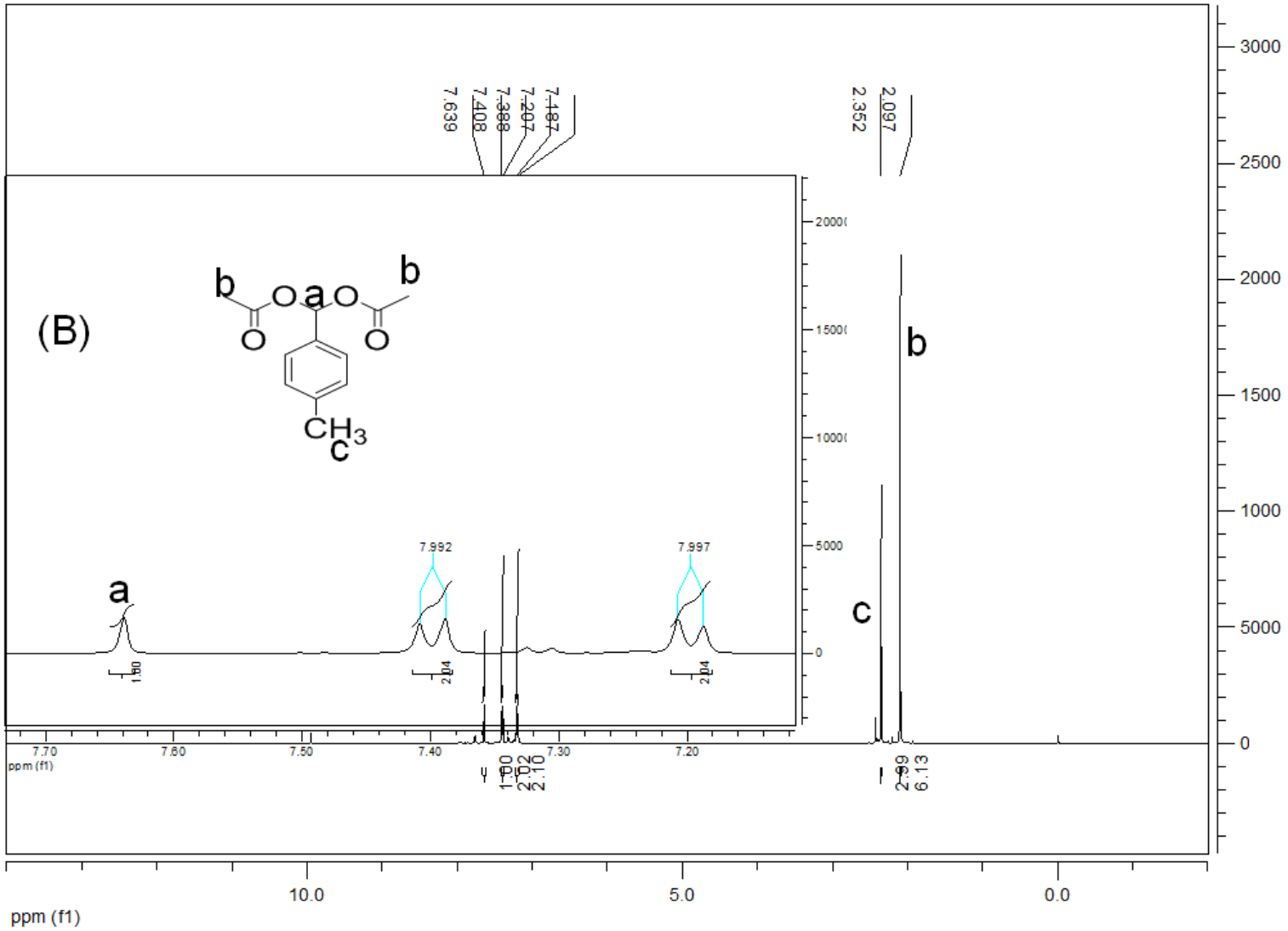

Fig. S5 (B) ^{1}H NMR spectra of entry **1**.

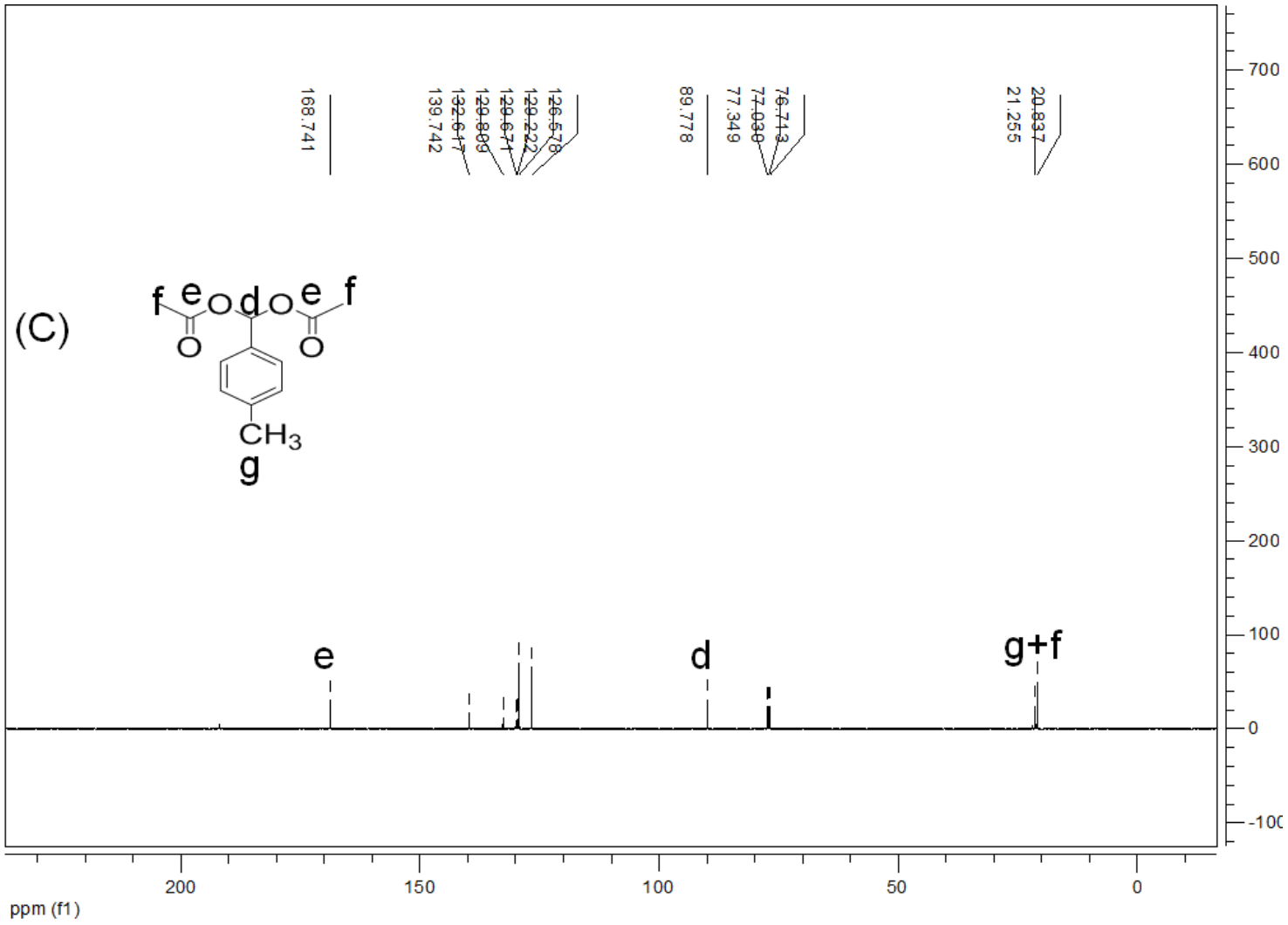

Fig. S5 (C) ^{13}C NMR spectra of entry **1**.

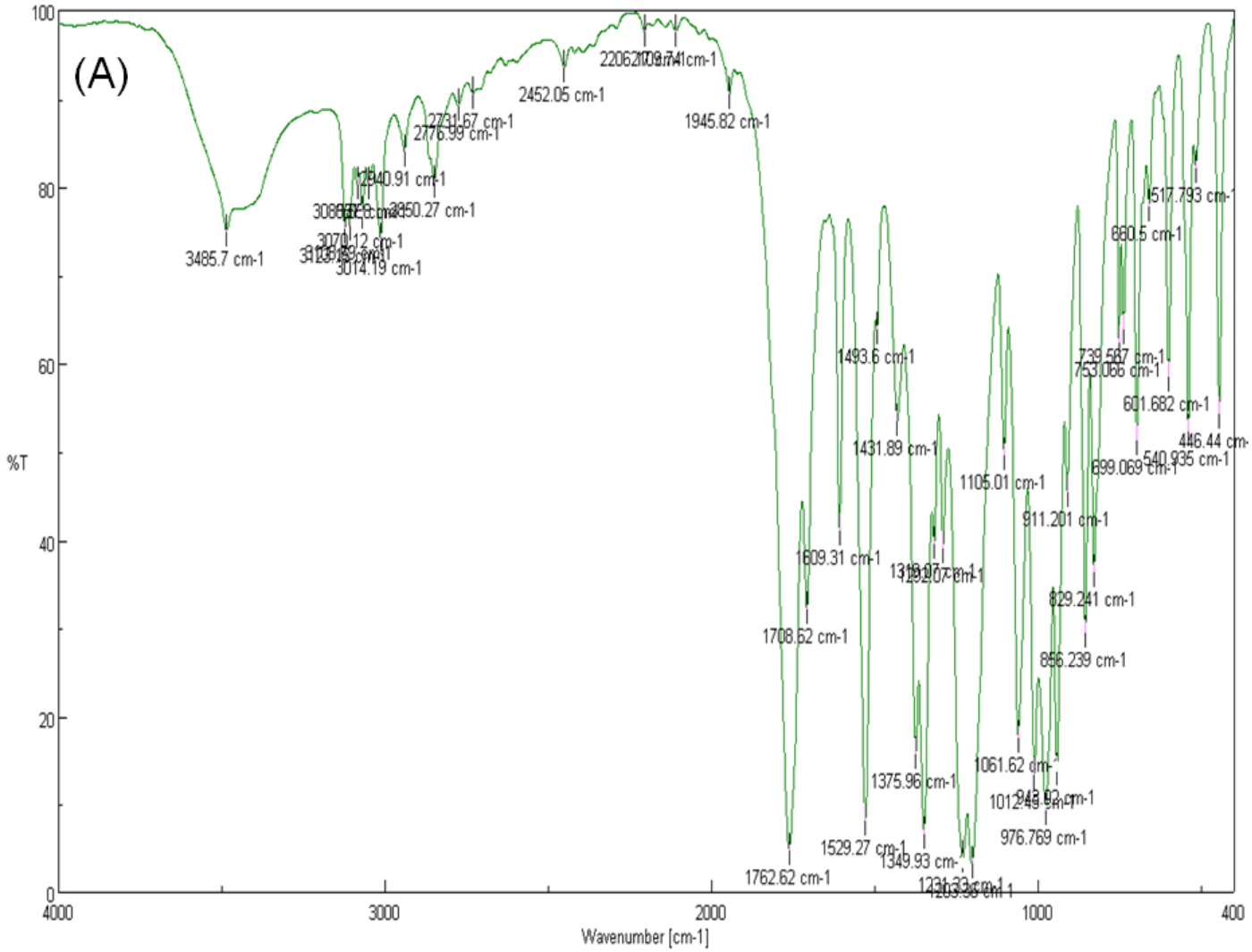

Fig. S6 (A) IR spectra of entry **2**.

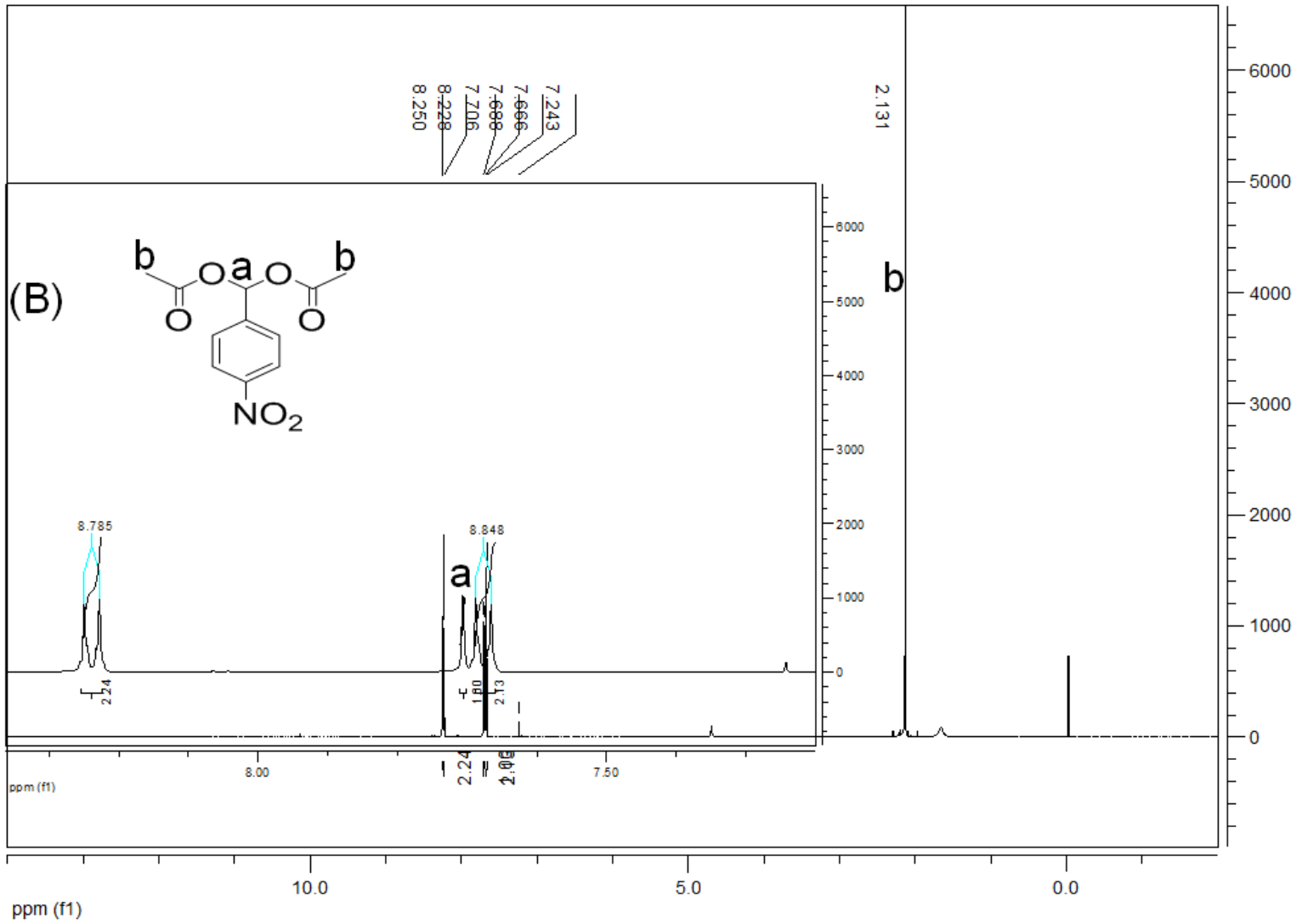

Fig. S6 (B) ^{1}H NMR spectra of entry **2**.

x

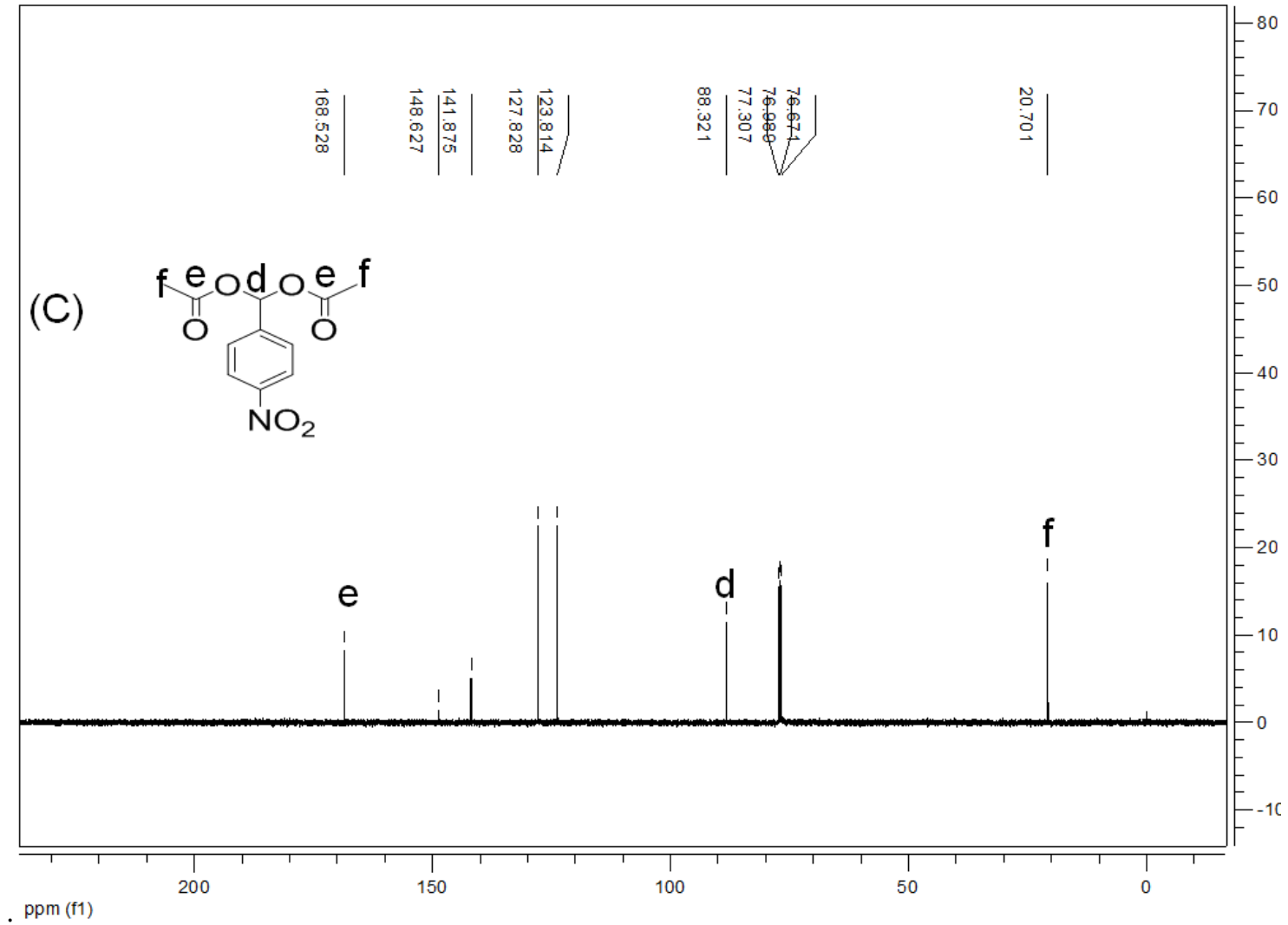

Fig. S6 (C) ^{13}C NMR spectra of entry **2**.

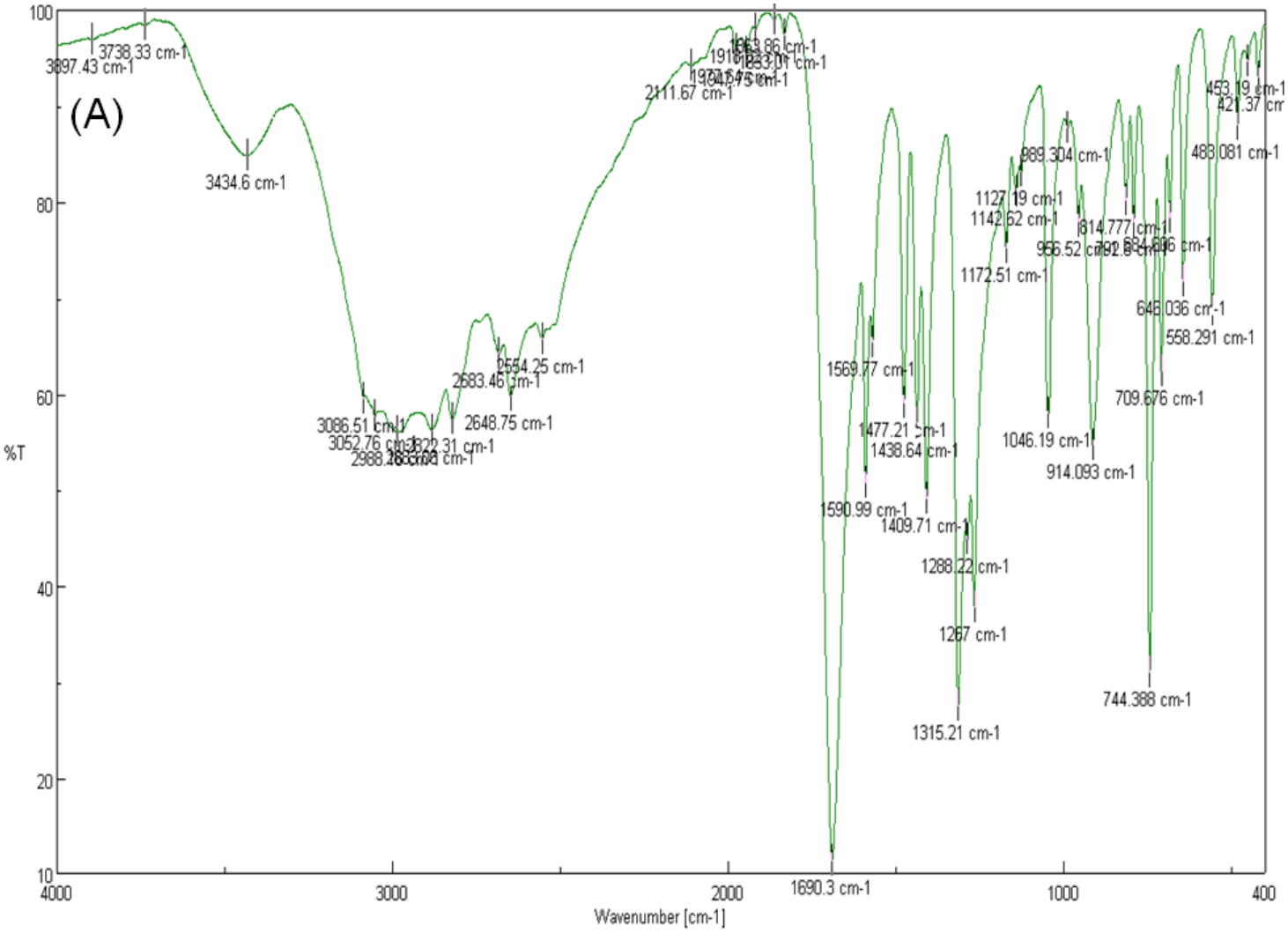

Fig. S7 (A) IR spectra of entry **3**.

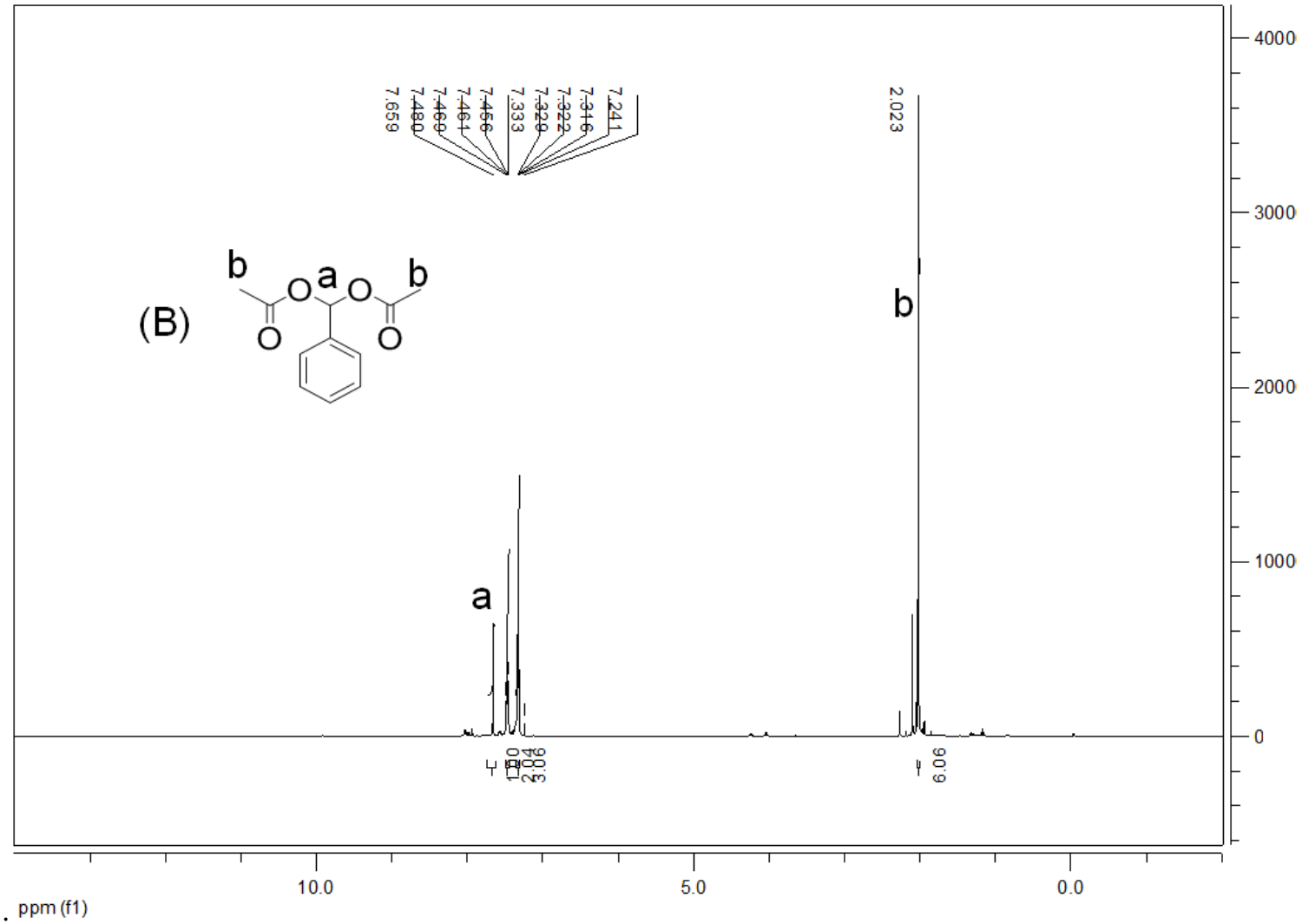

Fig. S7 (B) ^{1}H NMR spectra of entry **3**.

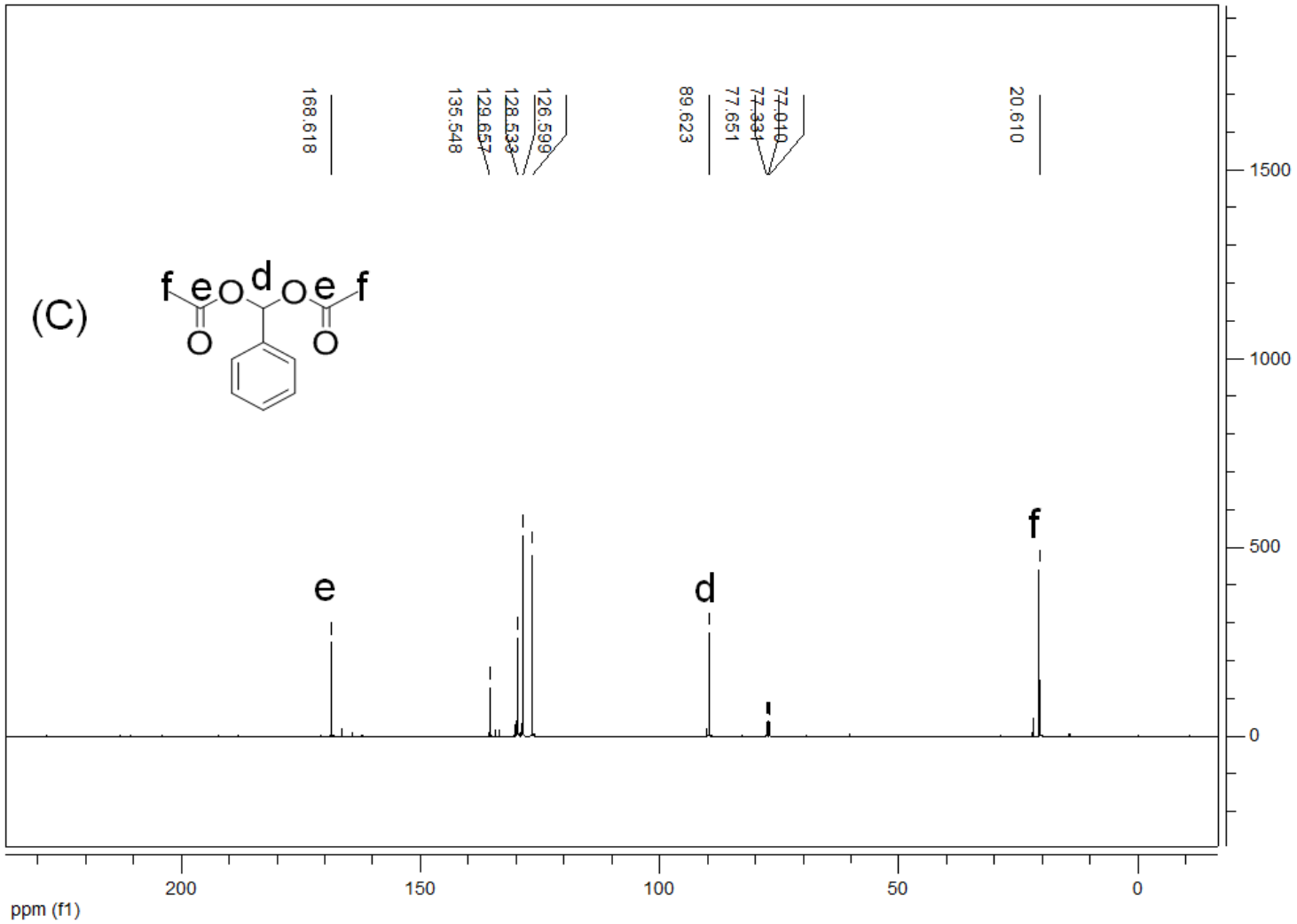

Fig. S7 (C) ^{13}C NMR spectra of entry **3**.

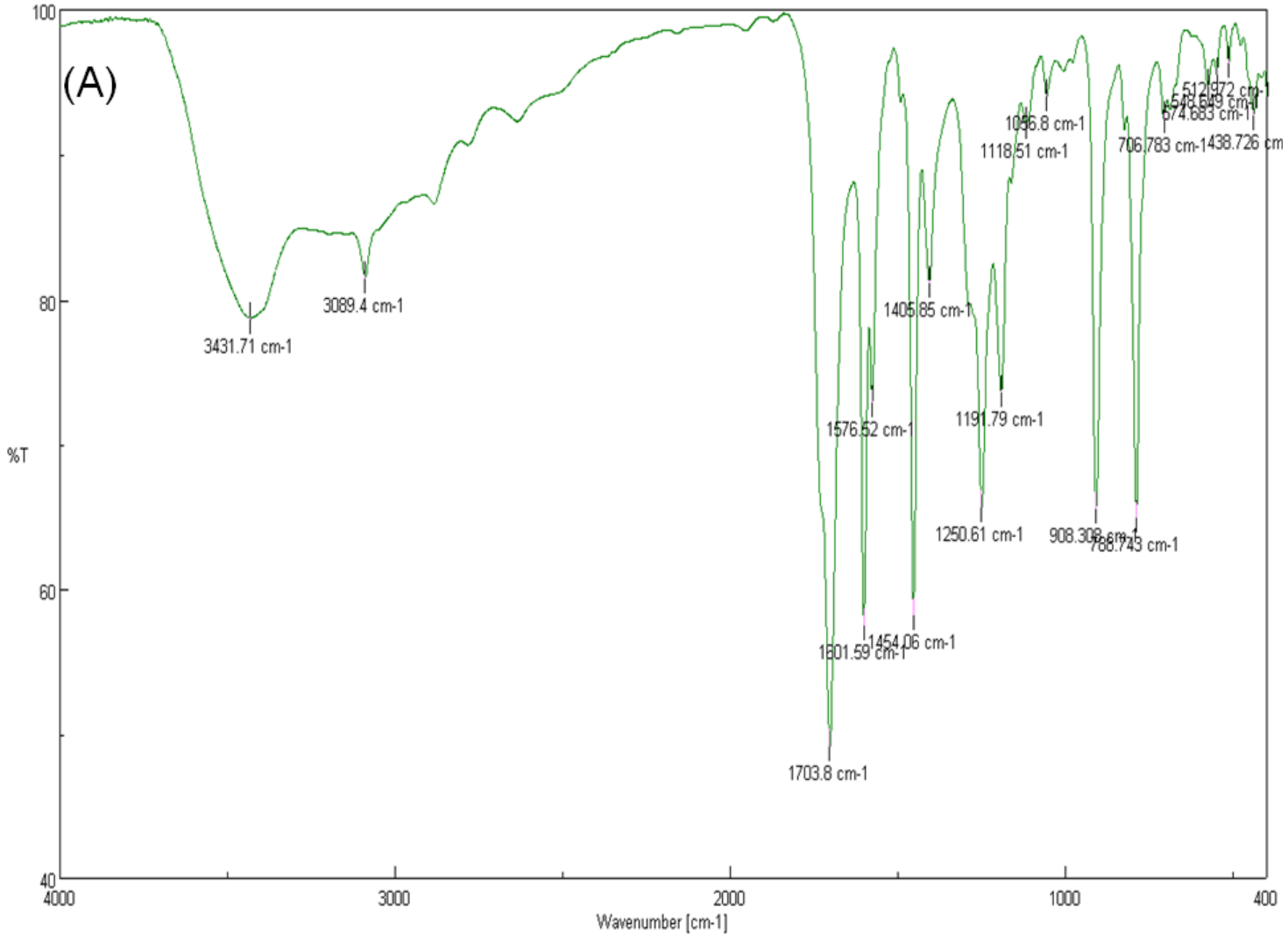

Fig. S8 (A) IR spectra of entry **4**.

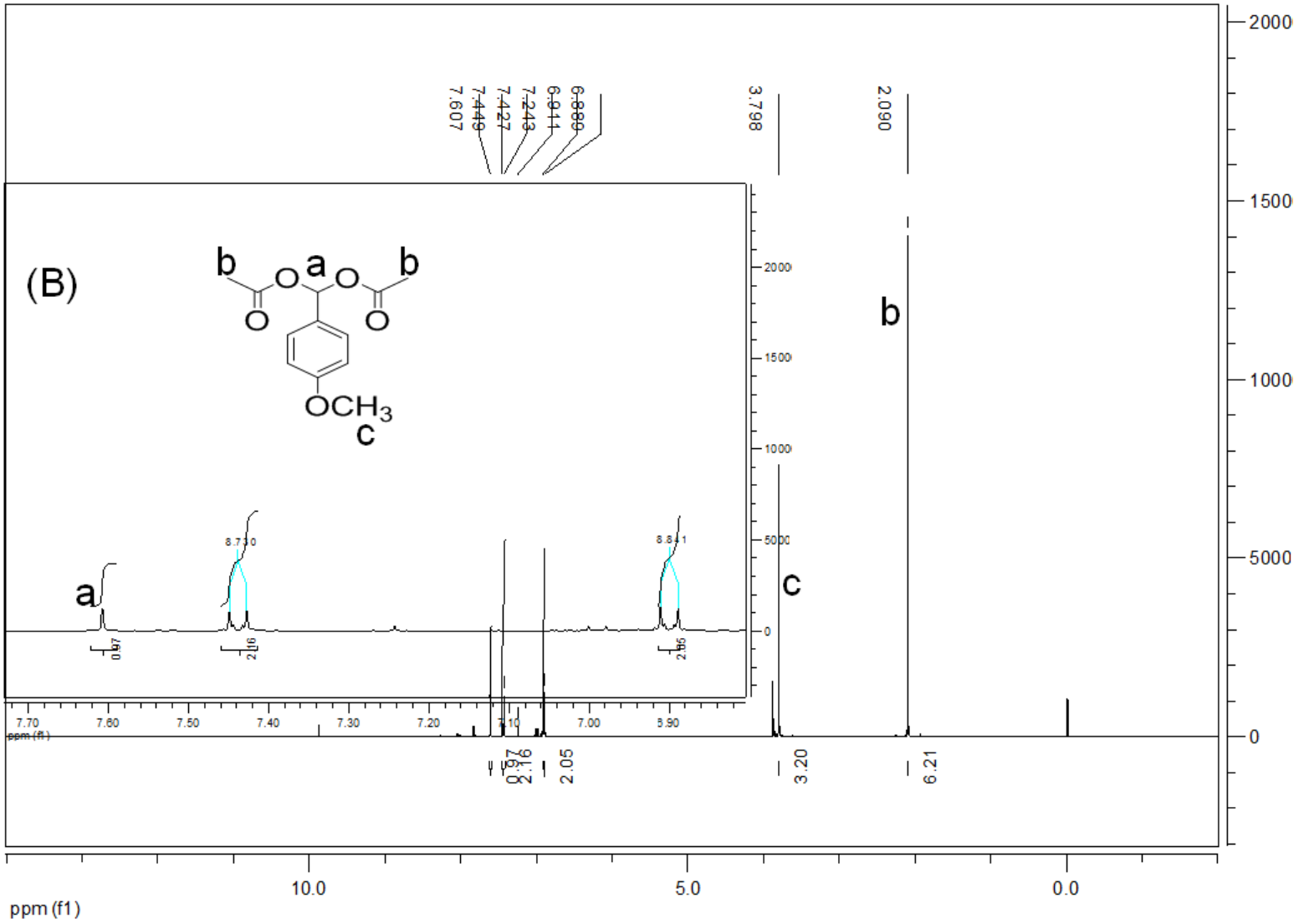

Fig. S8 (B) ^{1}H NMR spectra of entry **4**.

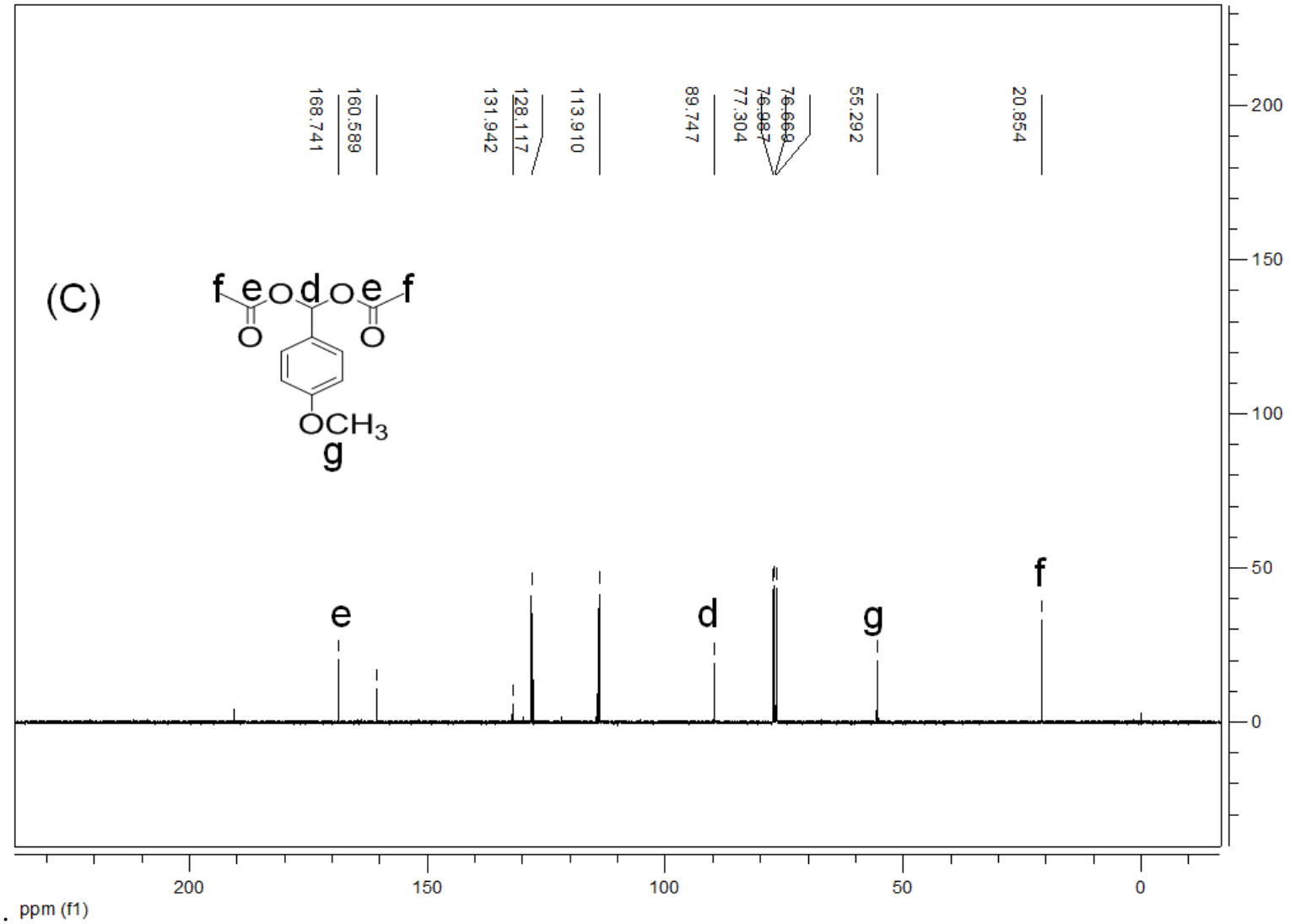

Fig. S8 (C) ^{13}C NMR spectra of entry **4**.

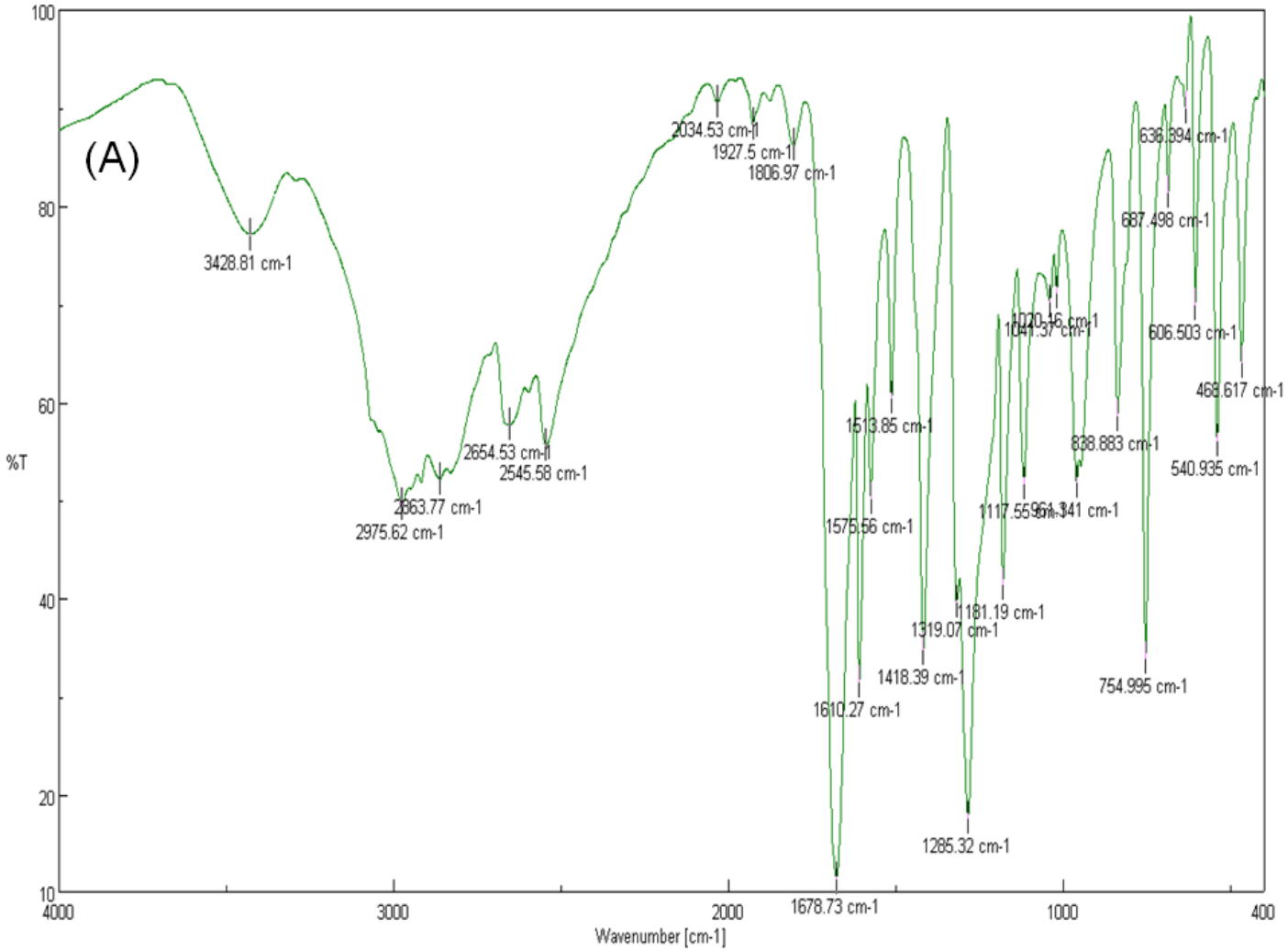

Fig. S9 (A) IR spectra of entry **5**.

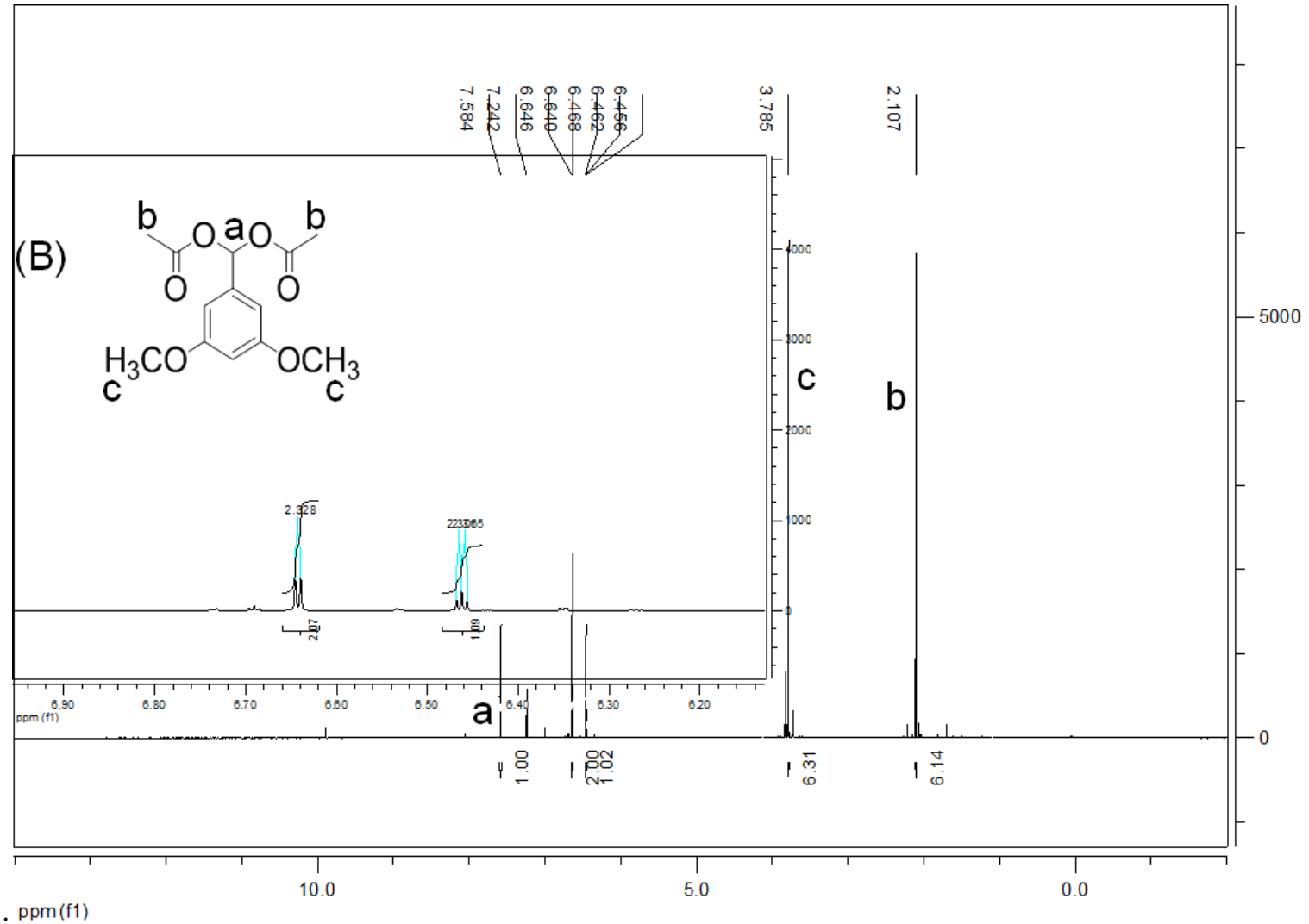

Fig. S9 (B) ^{1}H NMR spectra of entry **5**.

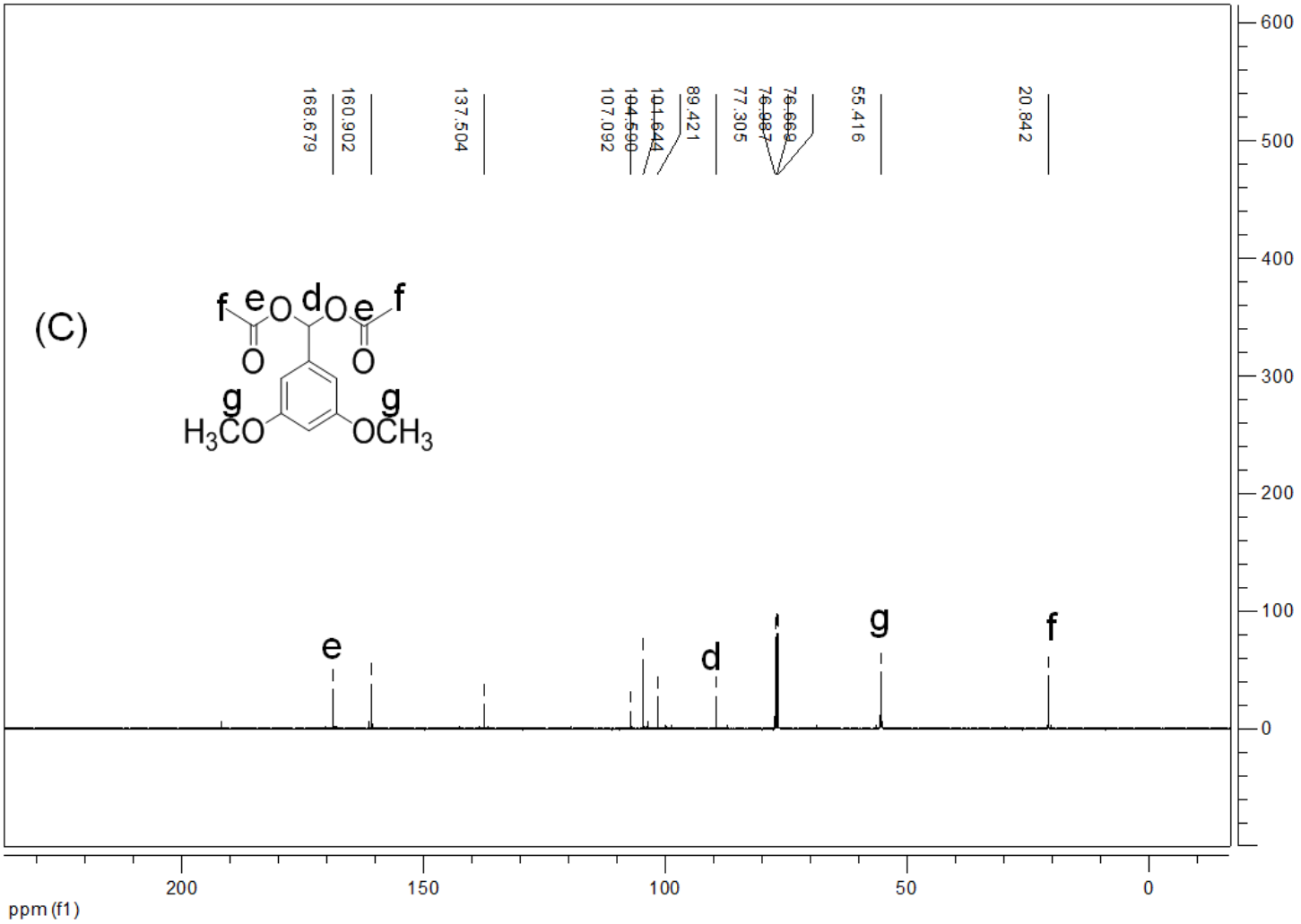

Fig. S9 (C) ^{13}C NMR spectra of entry **5**.

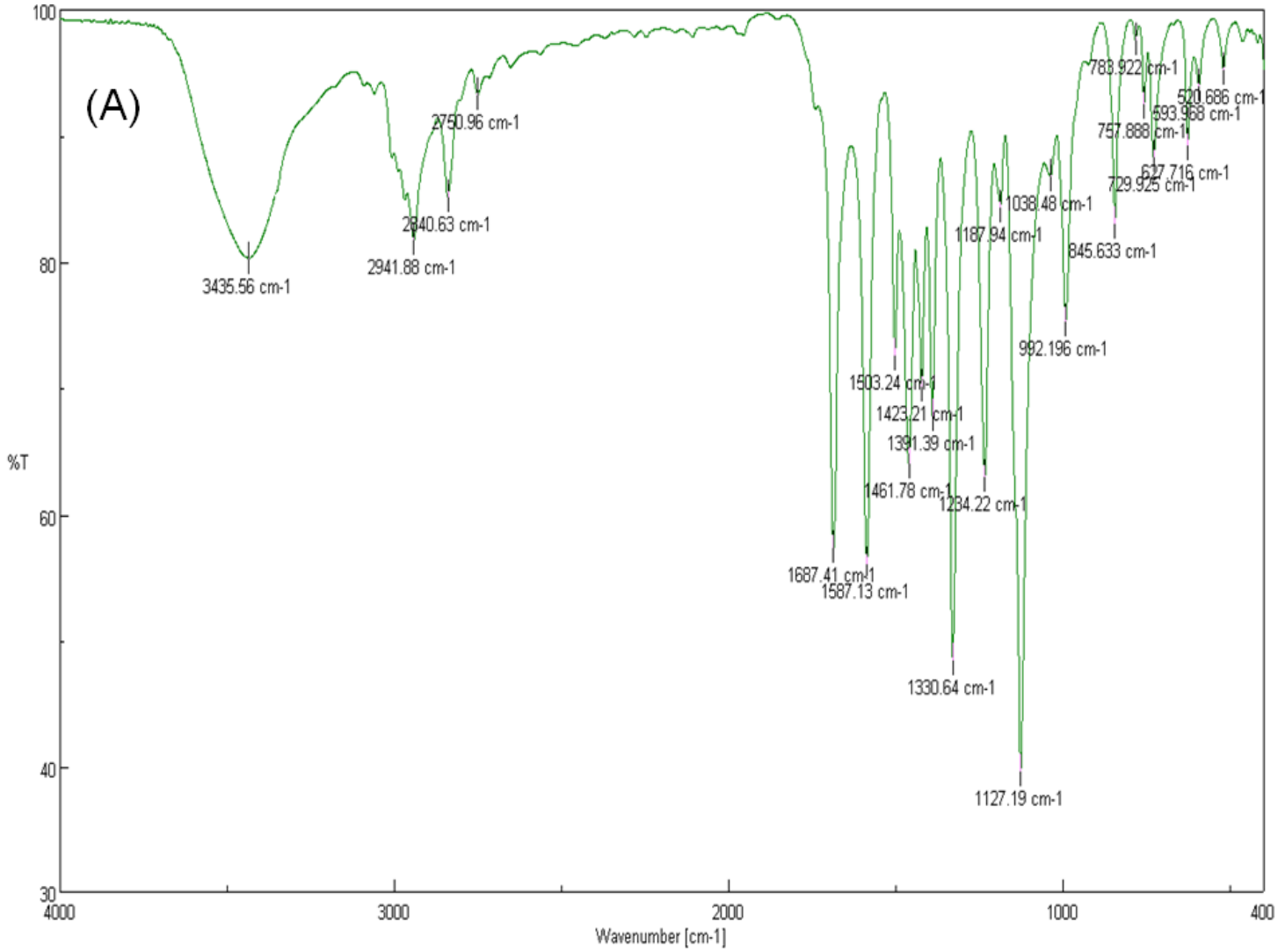

Fig. S10 (A) IR spectra of entry **6.**

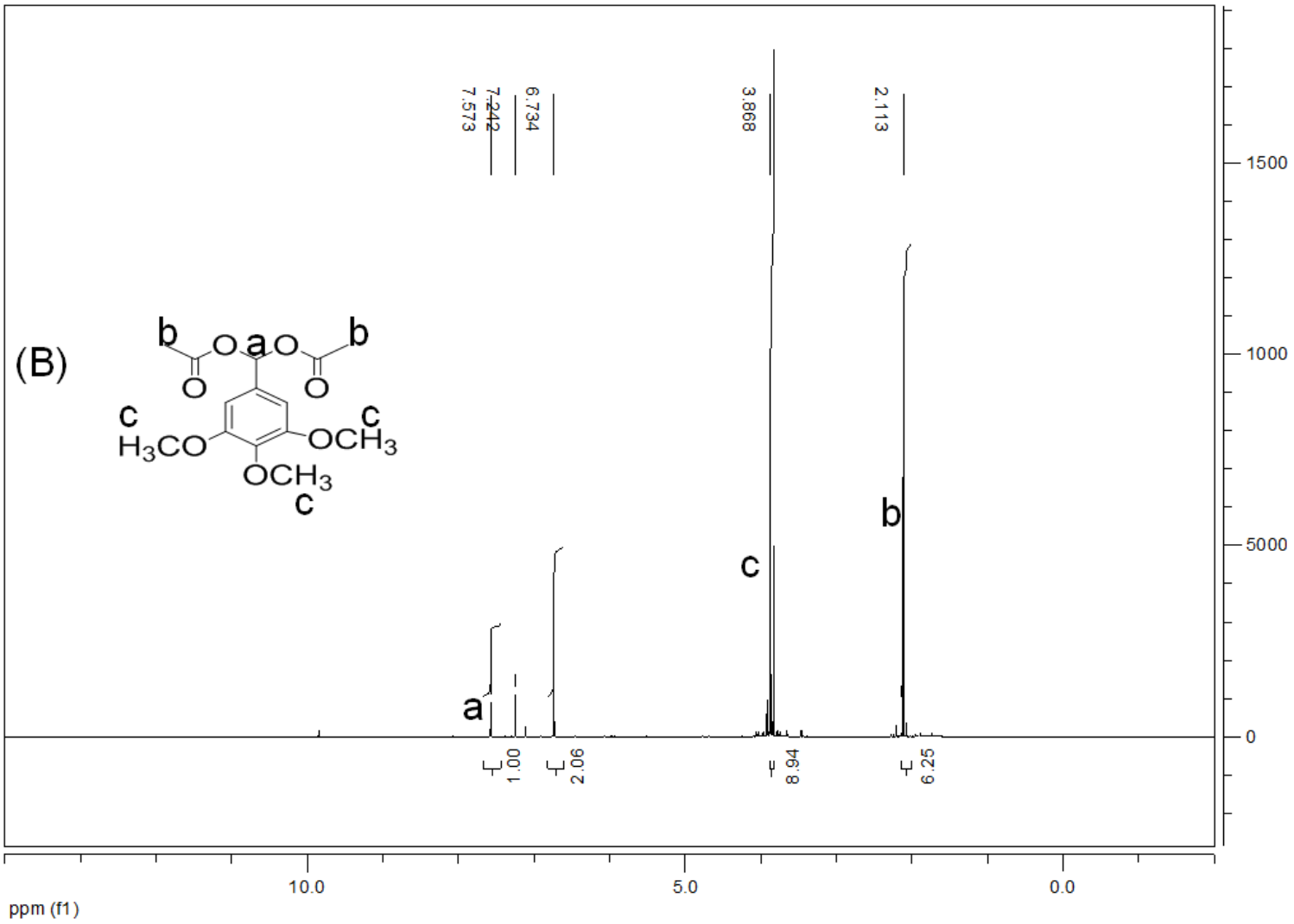

Fig. S10 (B) ^{1}H NMR spectra of entry **6.**

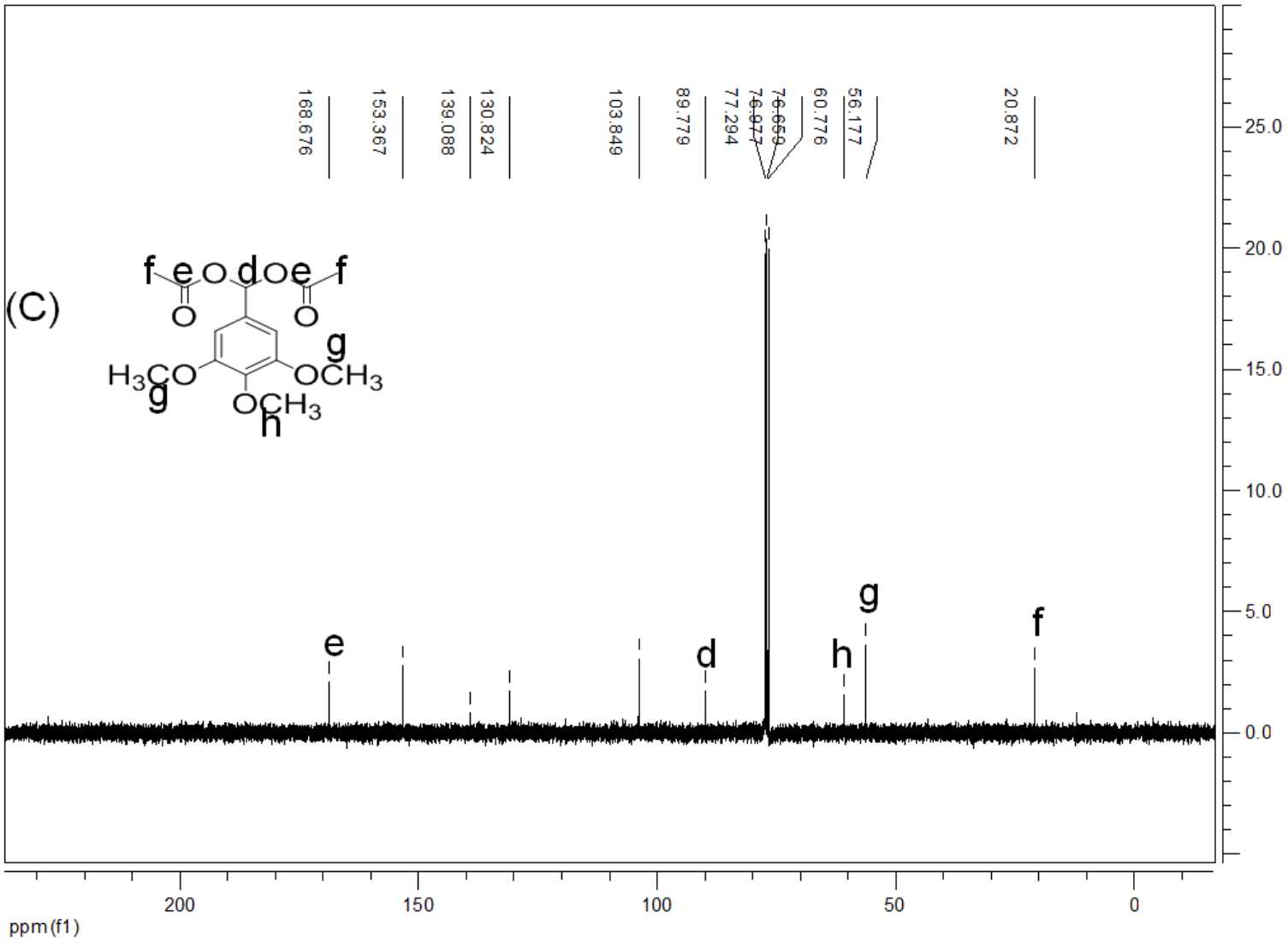

Fig. S10 (C) ^{13}C NMR spectra of entry **6.**

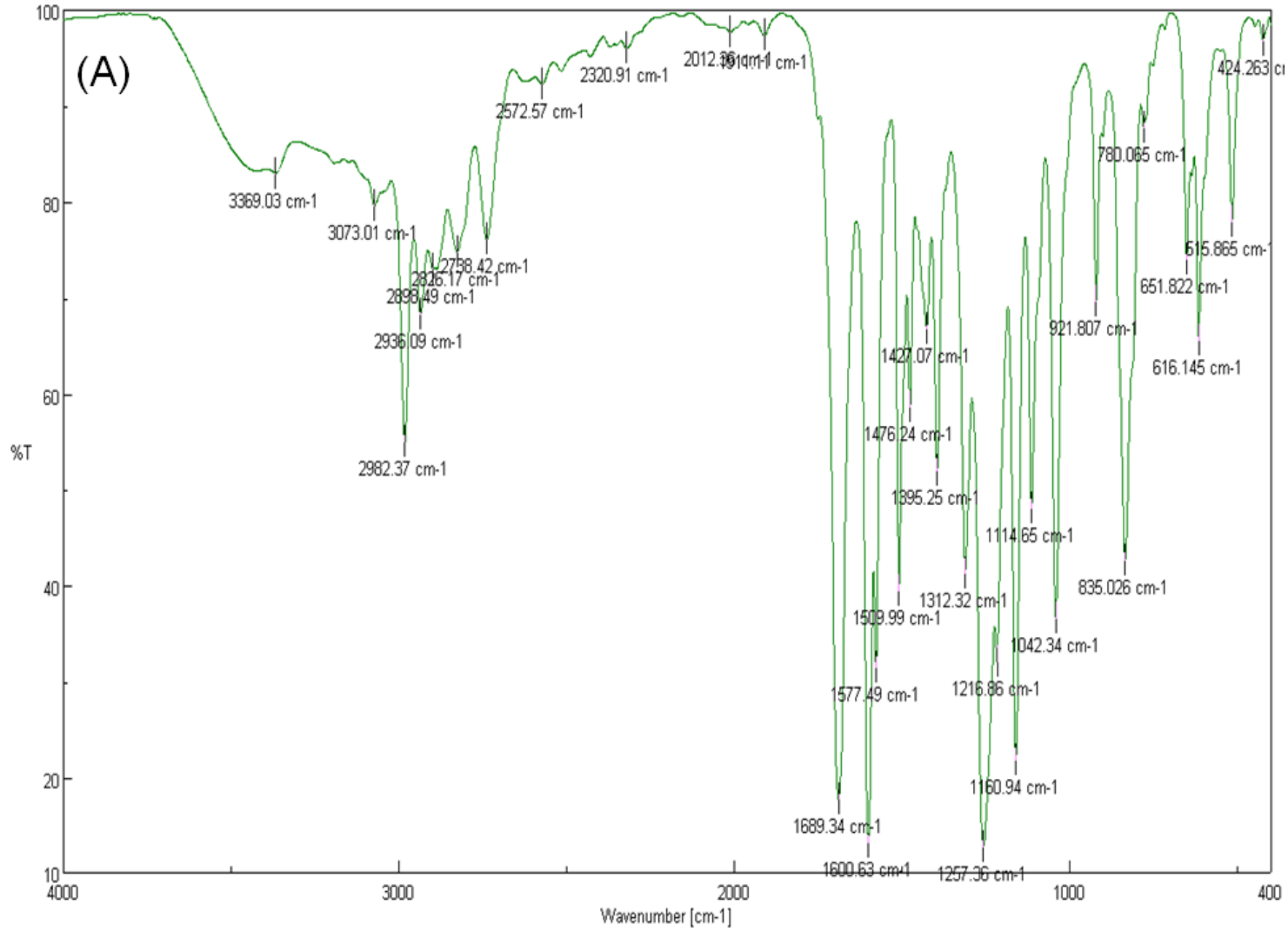

Fig. S11 (A) IR spectra of entry **7.**

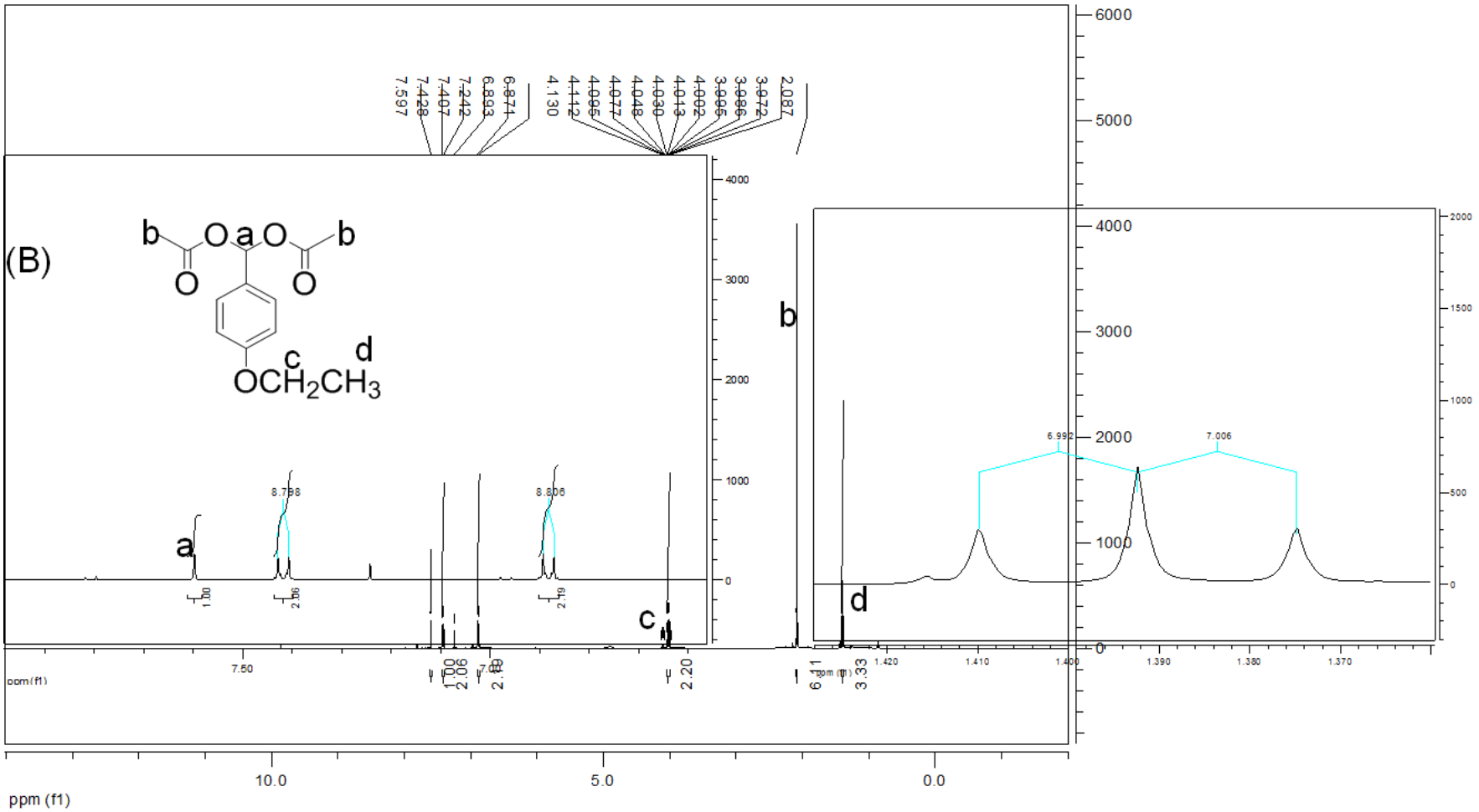

Fig. S11 (B) ^{1}H NMR spectra of entry **7.**

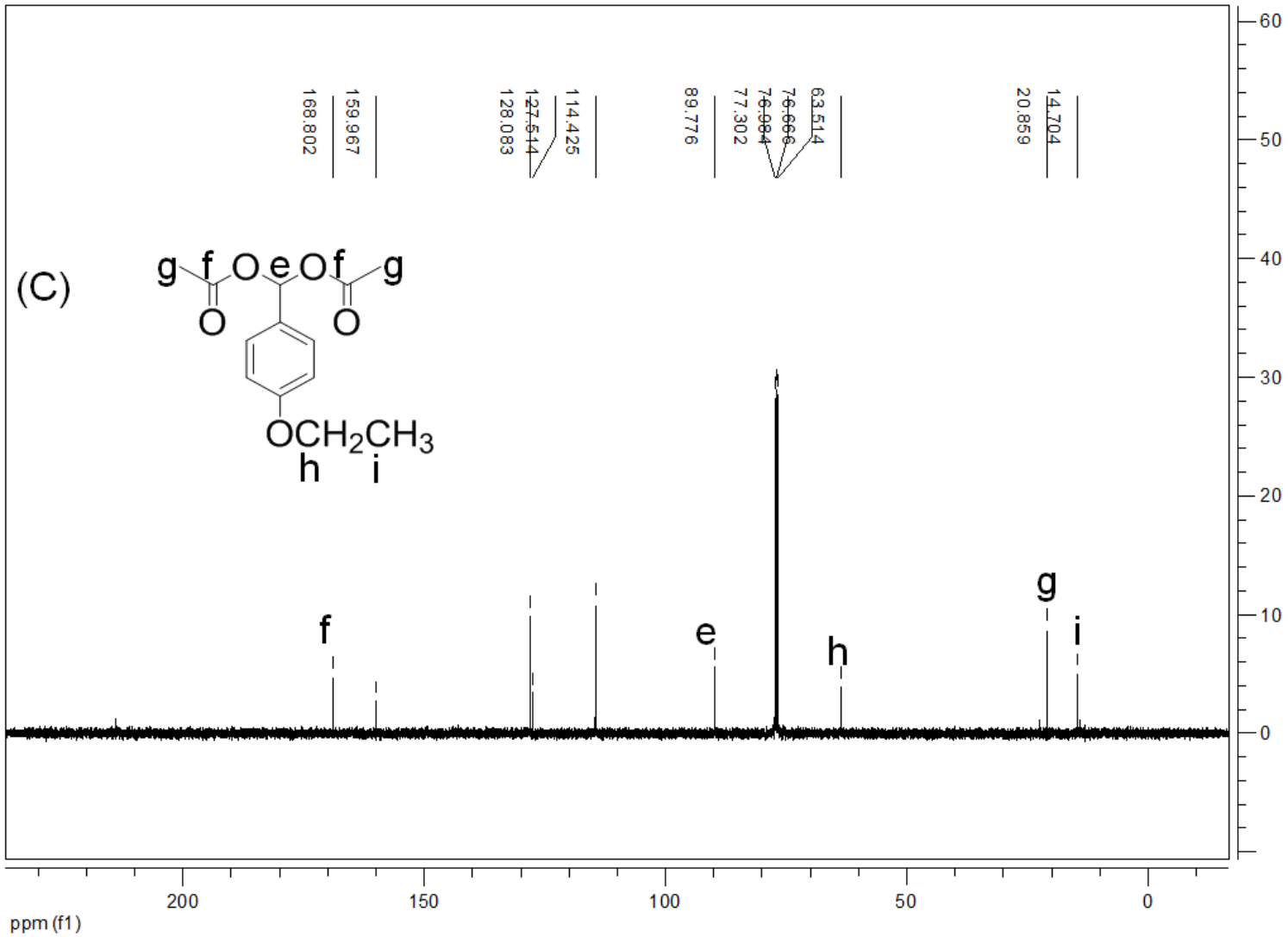

Fig. S11 (C) ^{13}C NMR spectra of entry **7.**

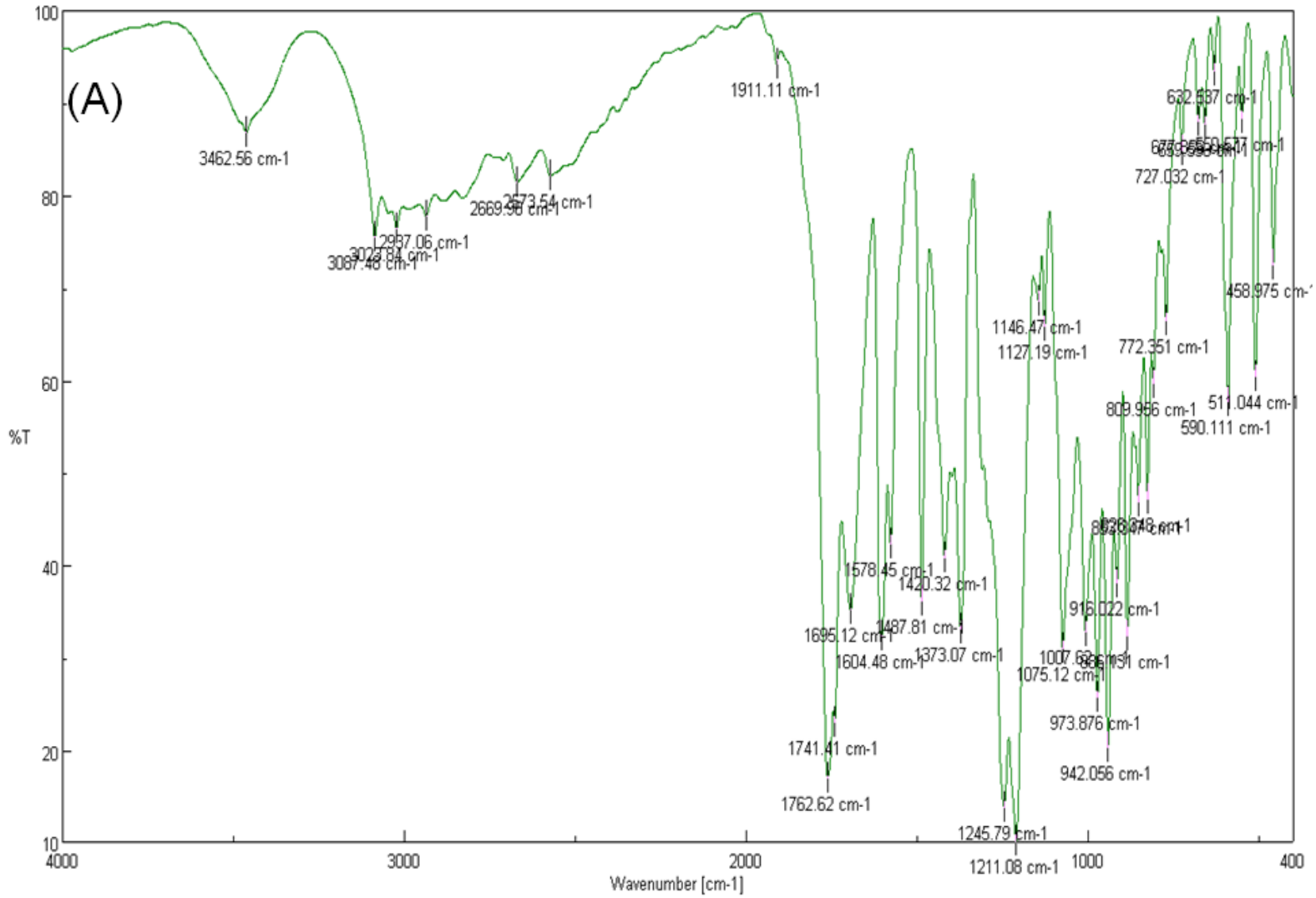

Fig. S12 (A) IR spectra of entry **8.**

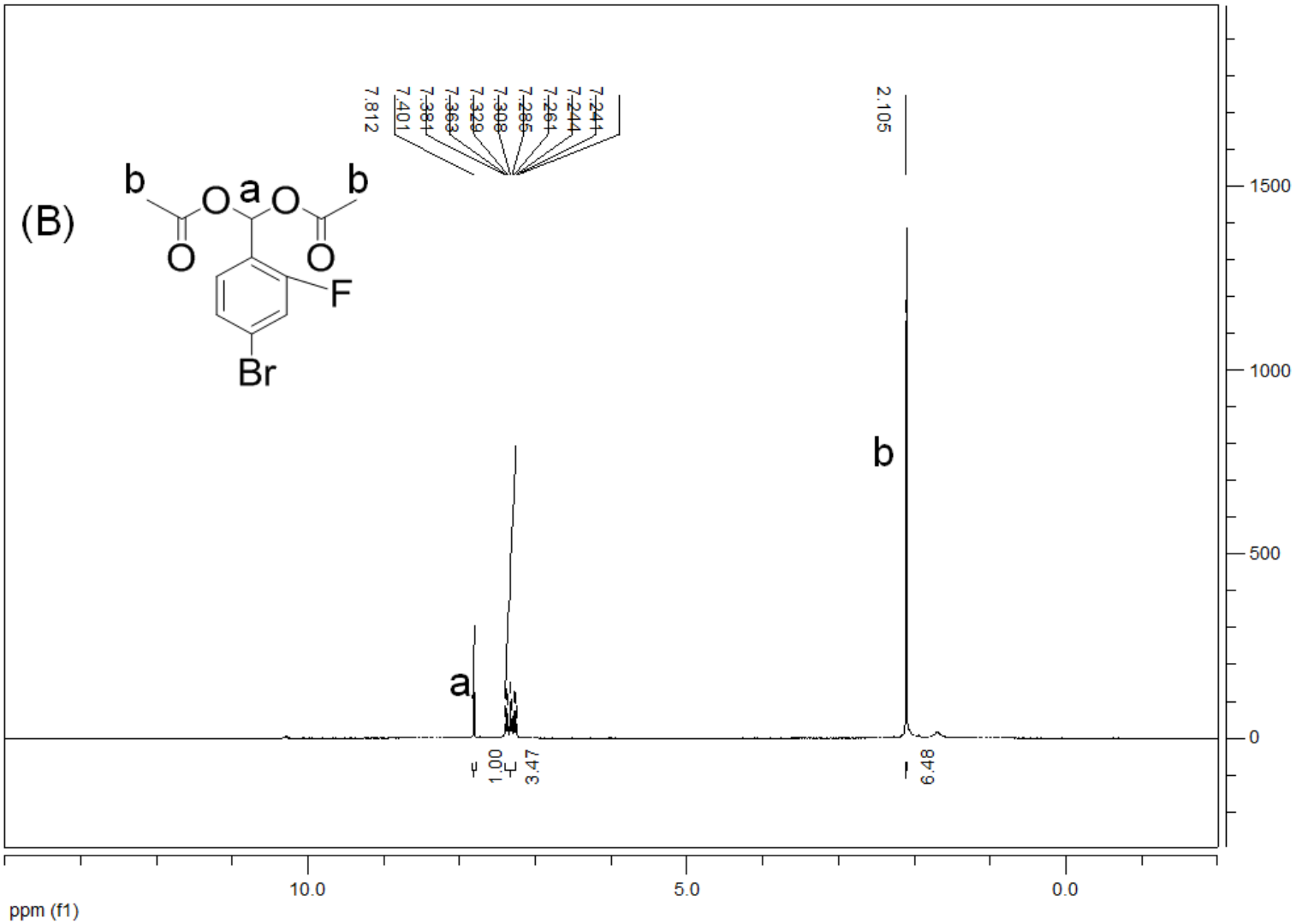

Fig. S12 (B) ^{1}H NMR spectra of entry **8.**

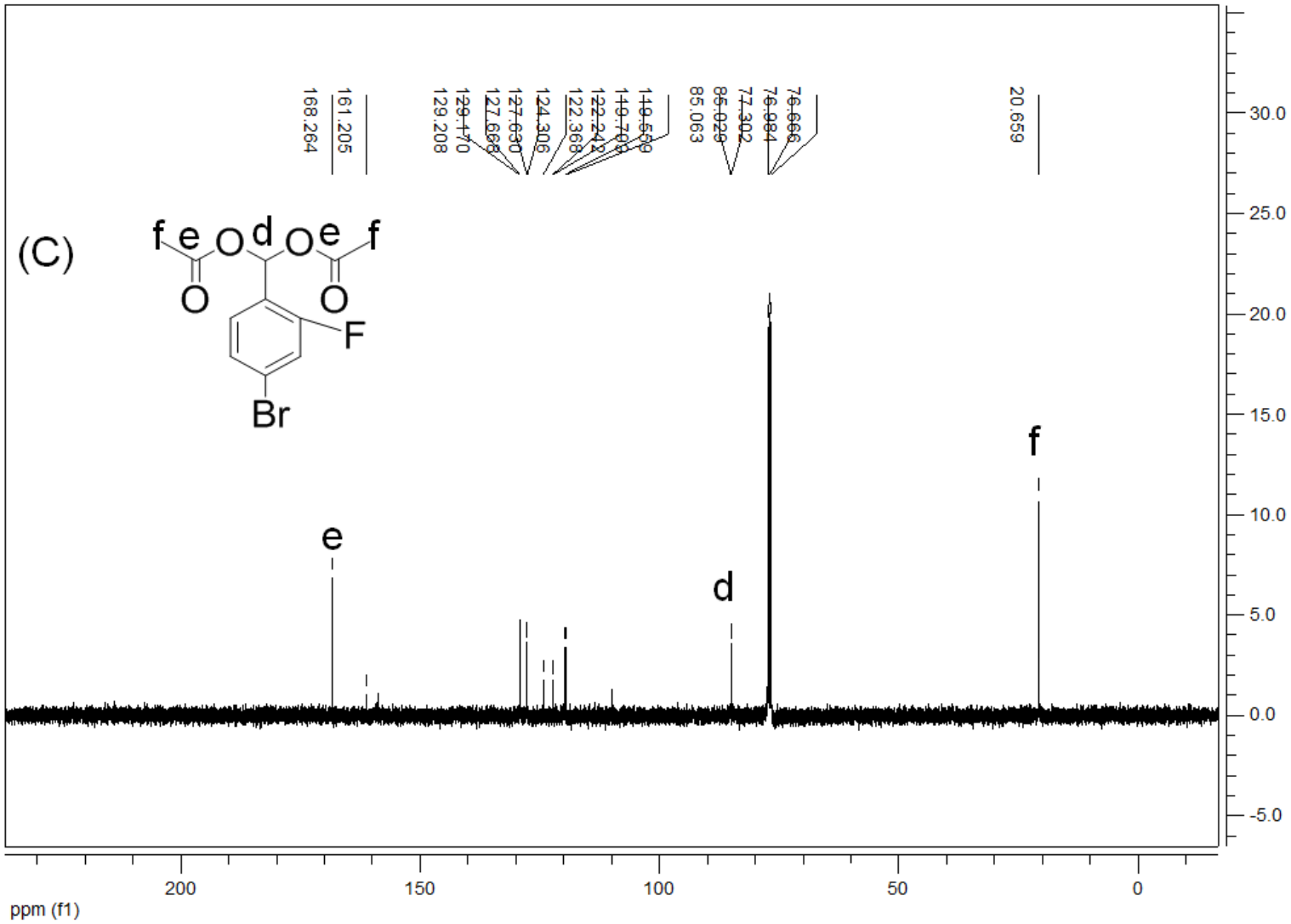

Fig. S12 (C) ^{13}C NMR spectra of entry **8.**

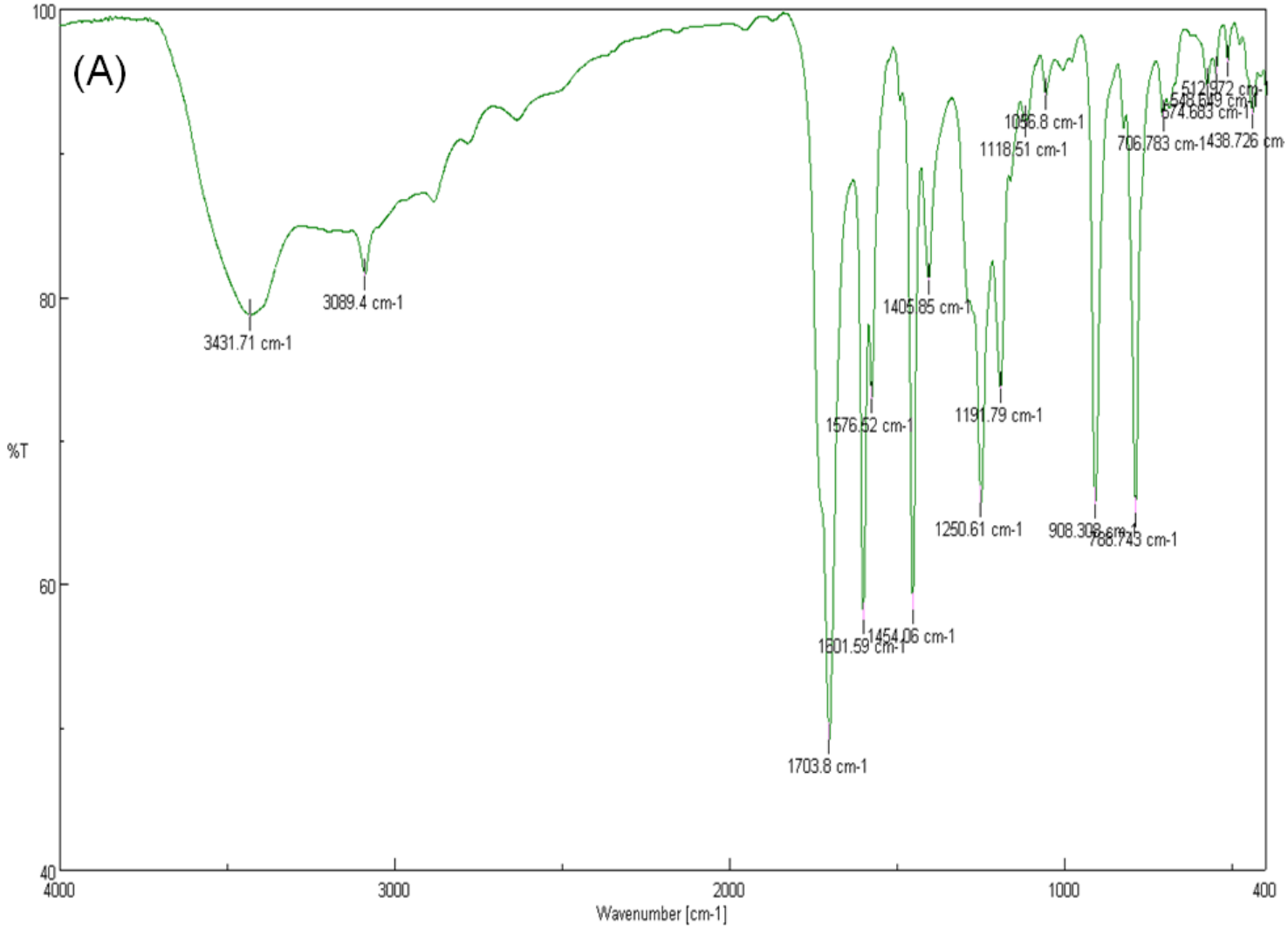

Fig. S13 (A) IR spectra of entry **9.**

xxx

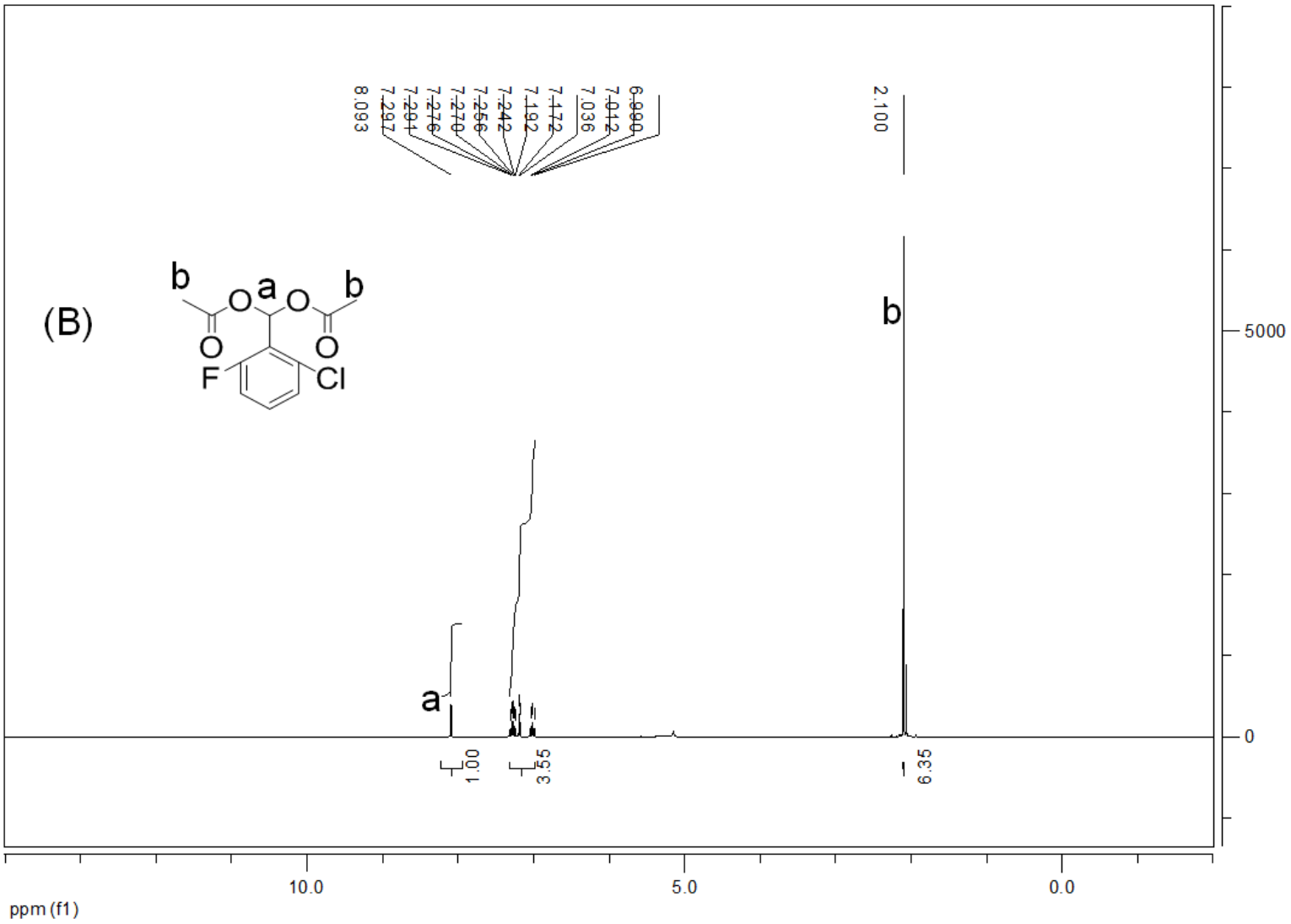

Fig. S13 (B) ^{1}H NMR spectra of entry **9.**

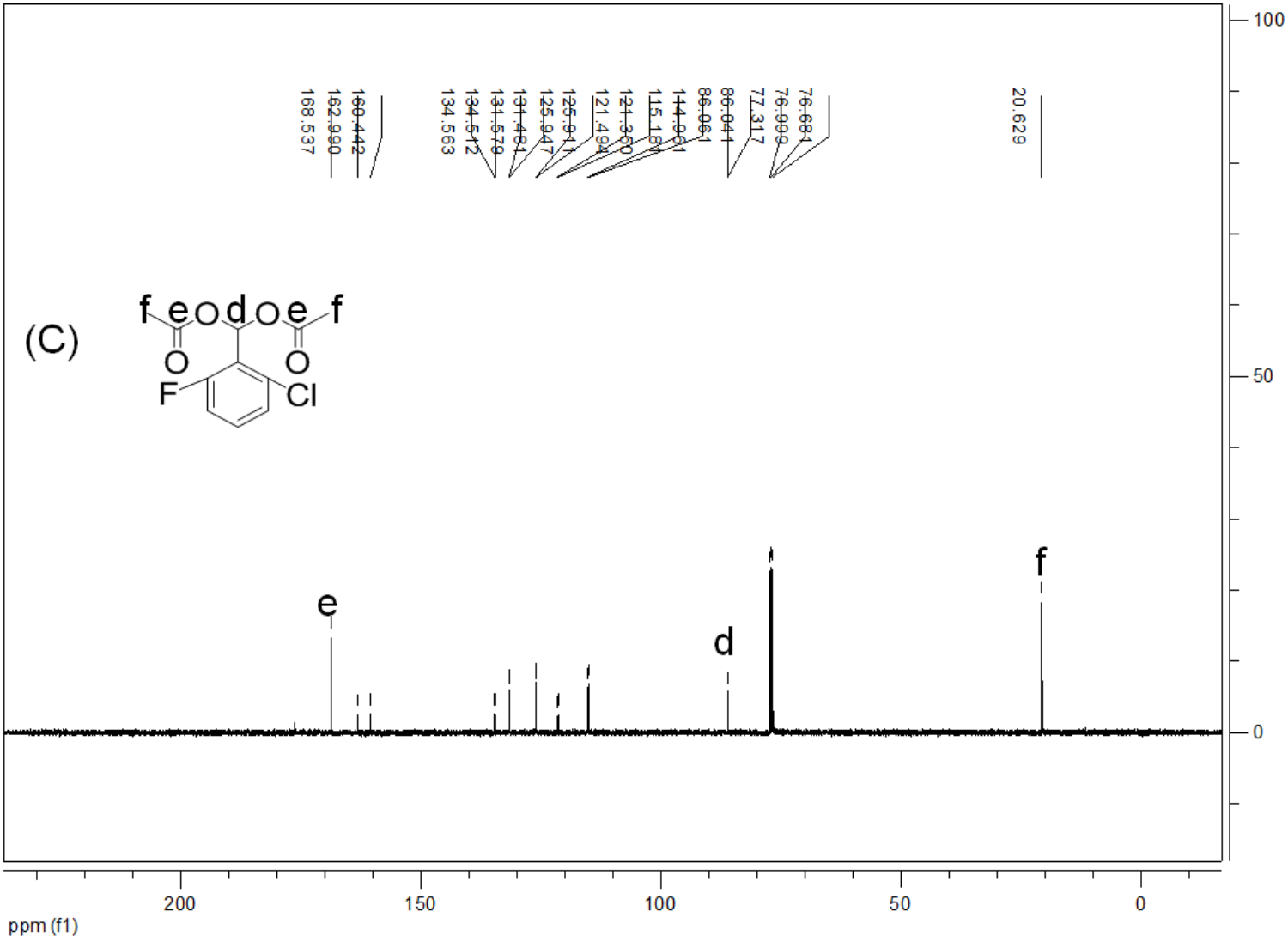

Fig. S13 (C) ^{13}C NMR spectra of entry **9.**

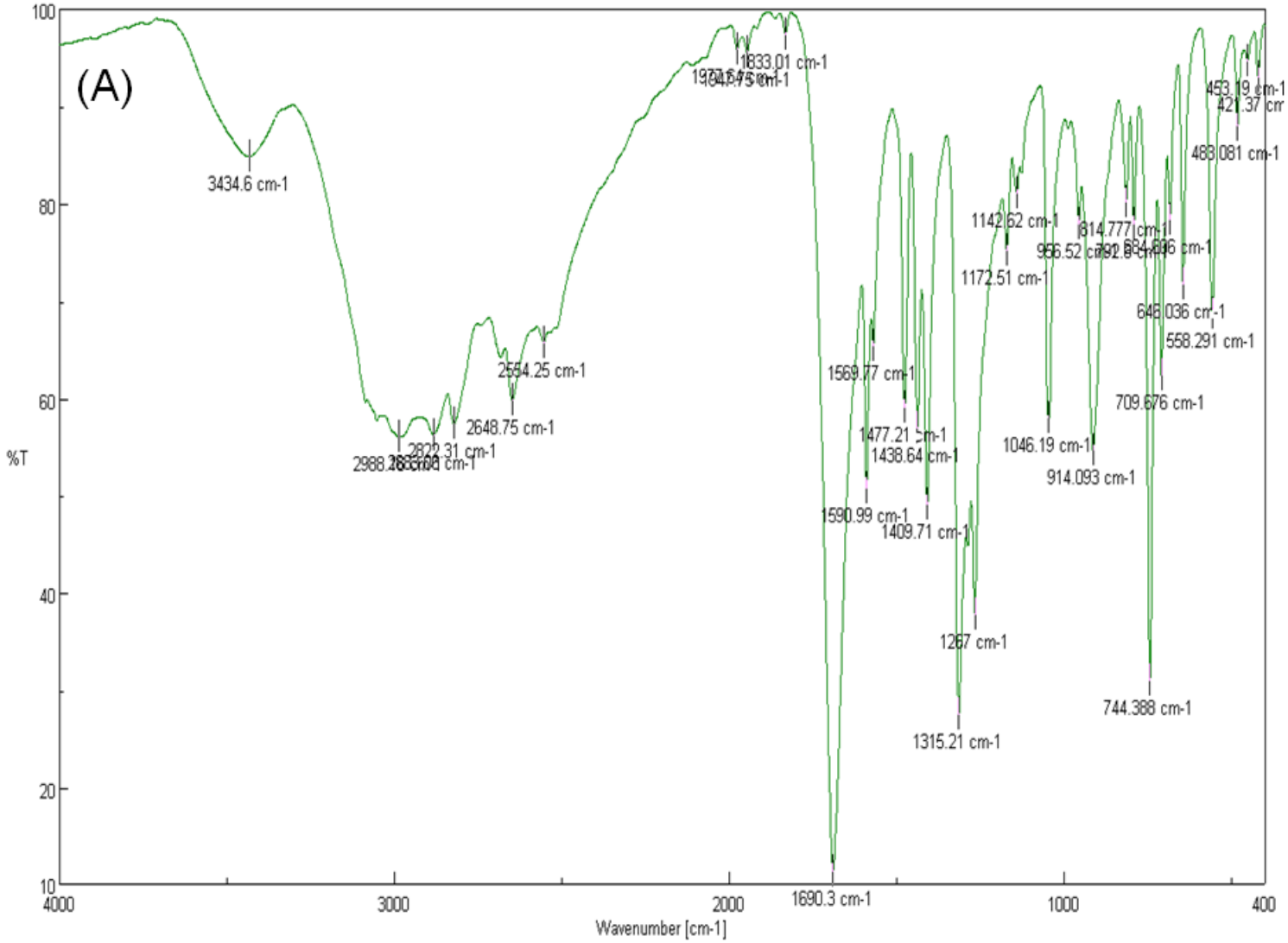

Fig. S14 (A) IR spectra of entry **10.**

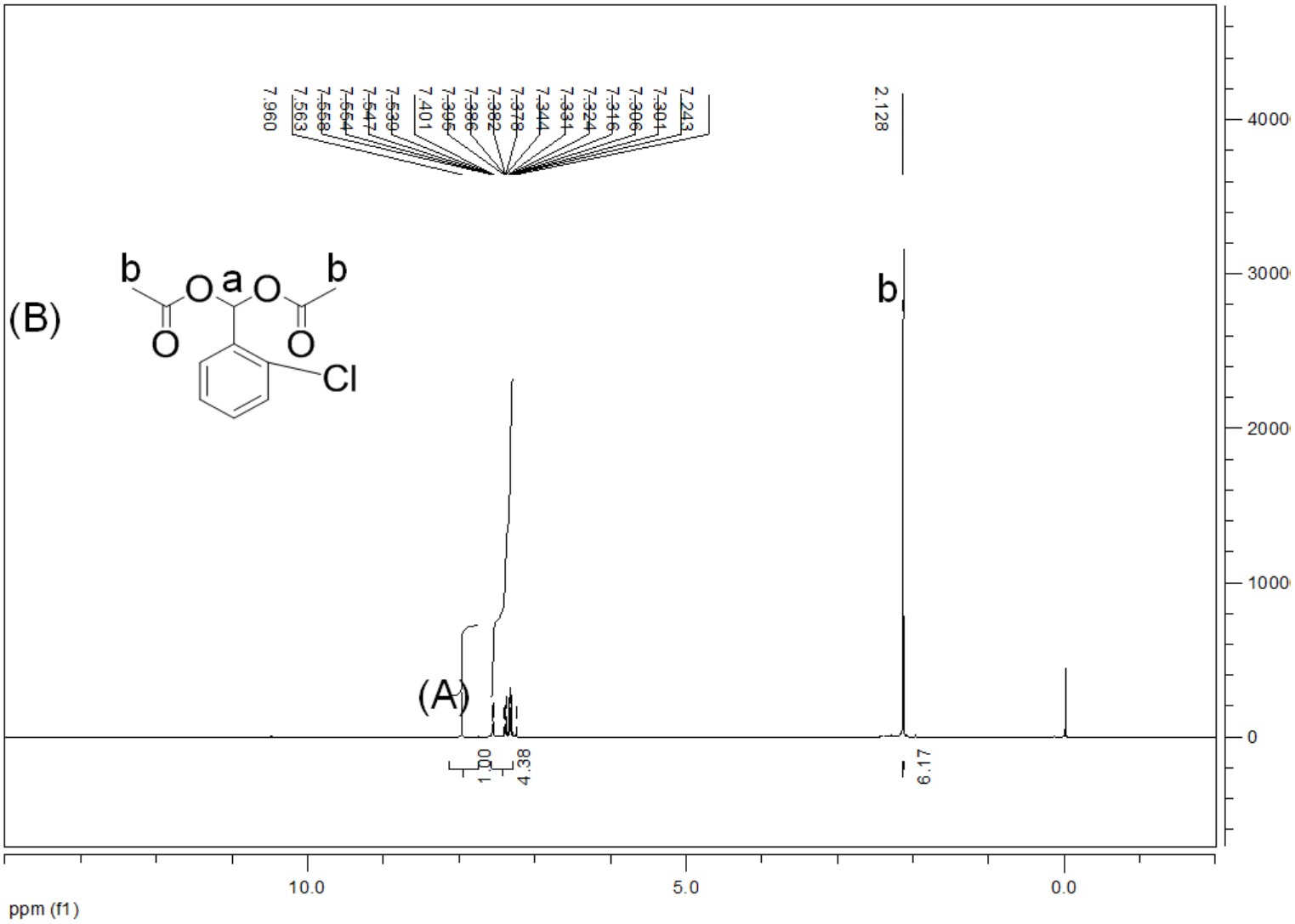

Fig. S14 (B) ^{1}H NMR spectra of entry **10.**

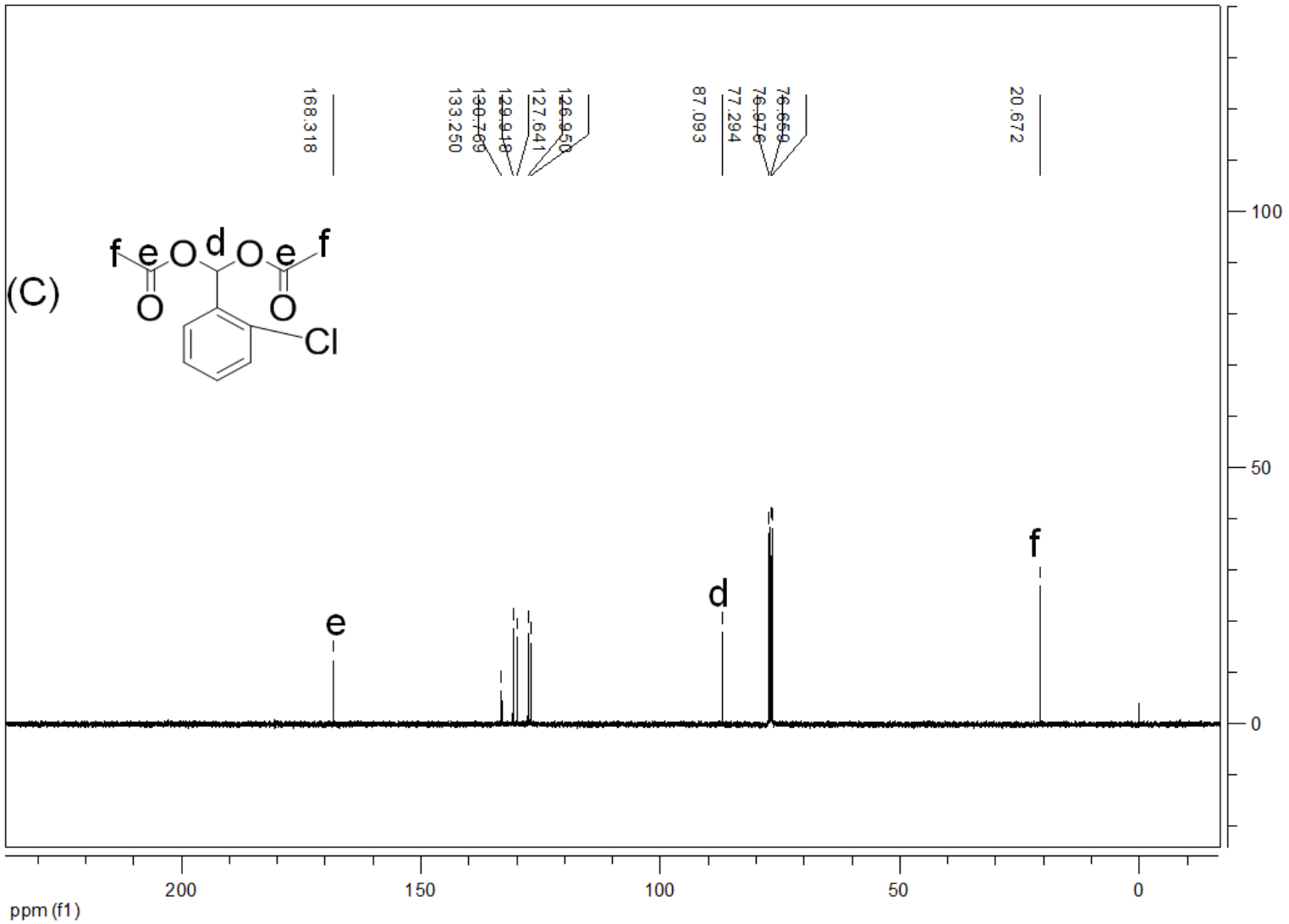

Fig. S14 (C) ^{13}C NMR spectra of entry **10.**

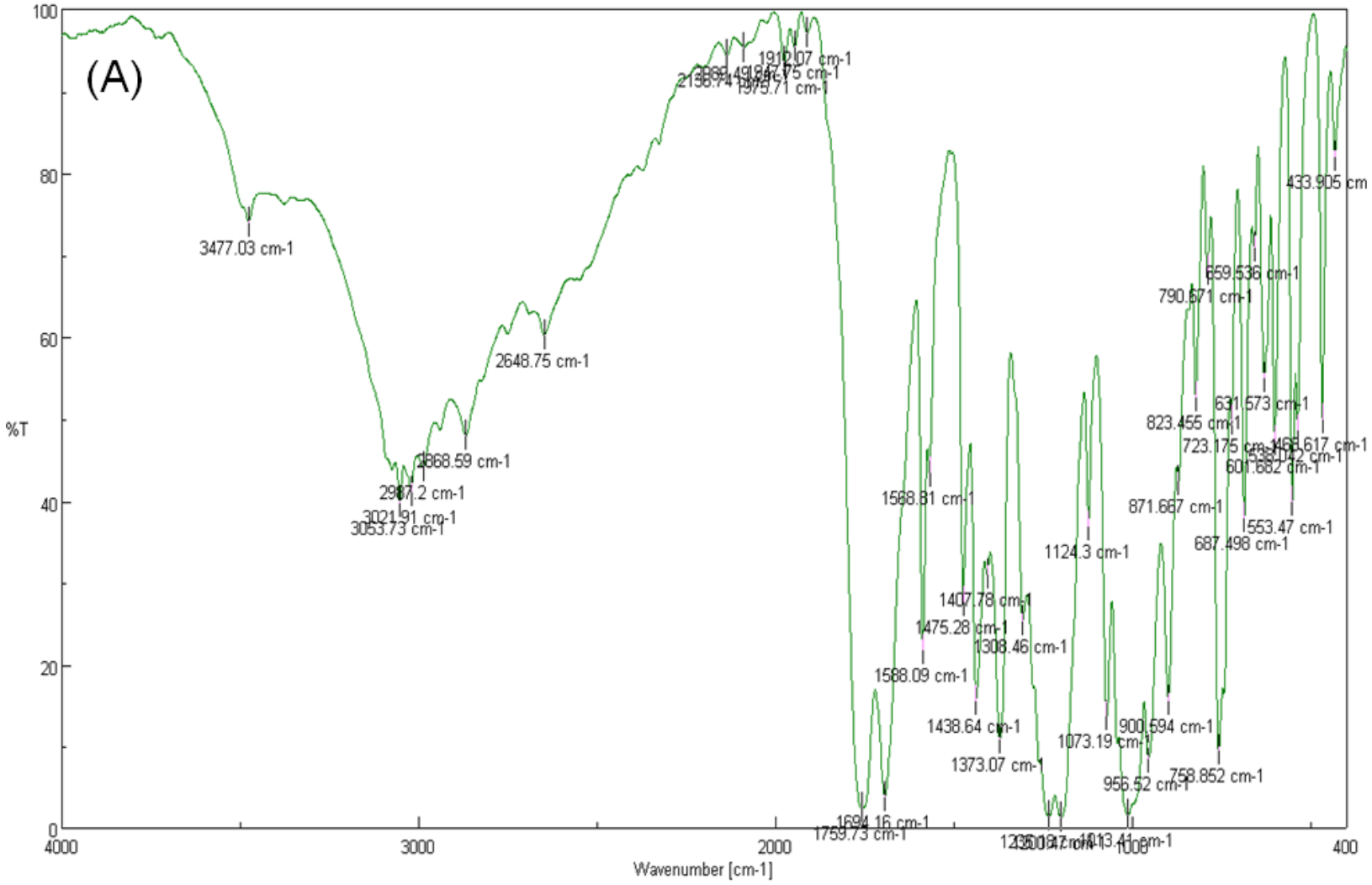

Fig. S15 (A) IR spectra of entry **11.**

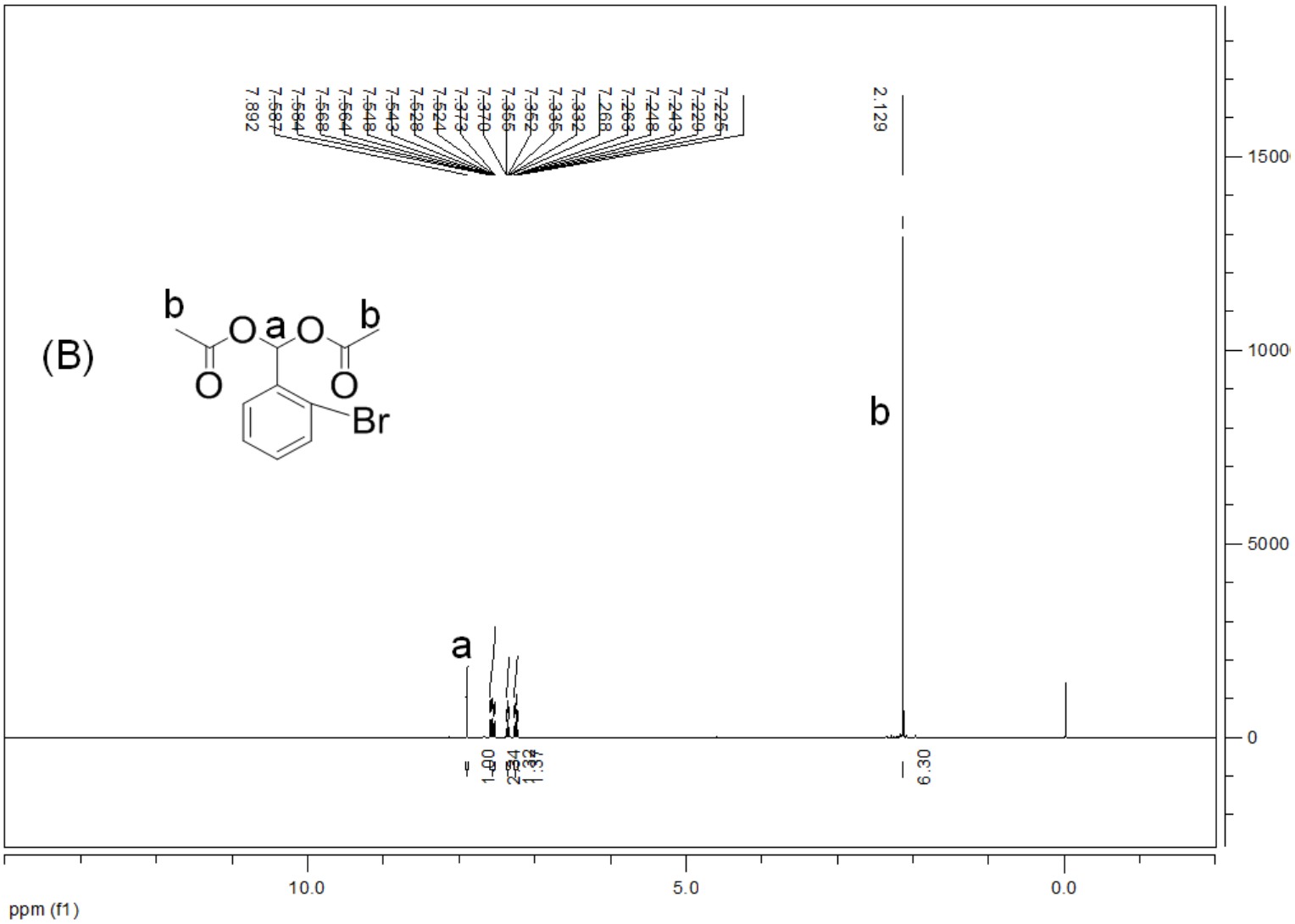

Fig. S15 (B) ^{1}H NMR spectra of entry **11.**

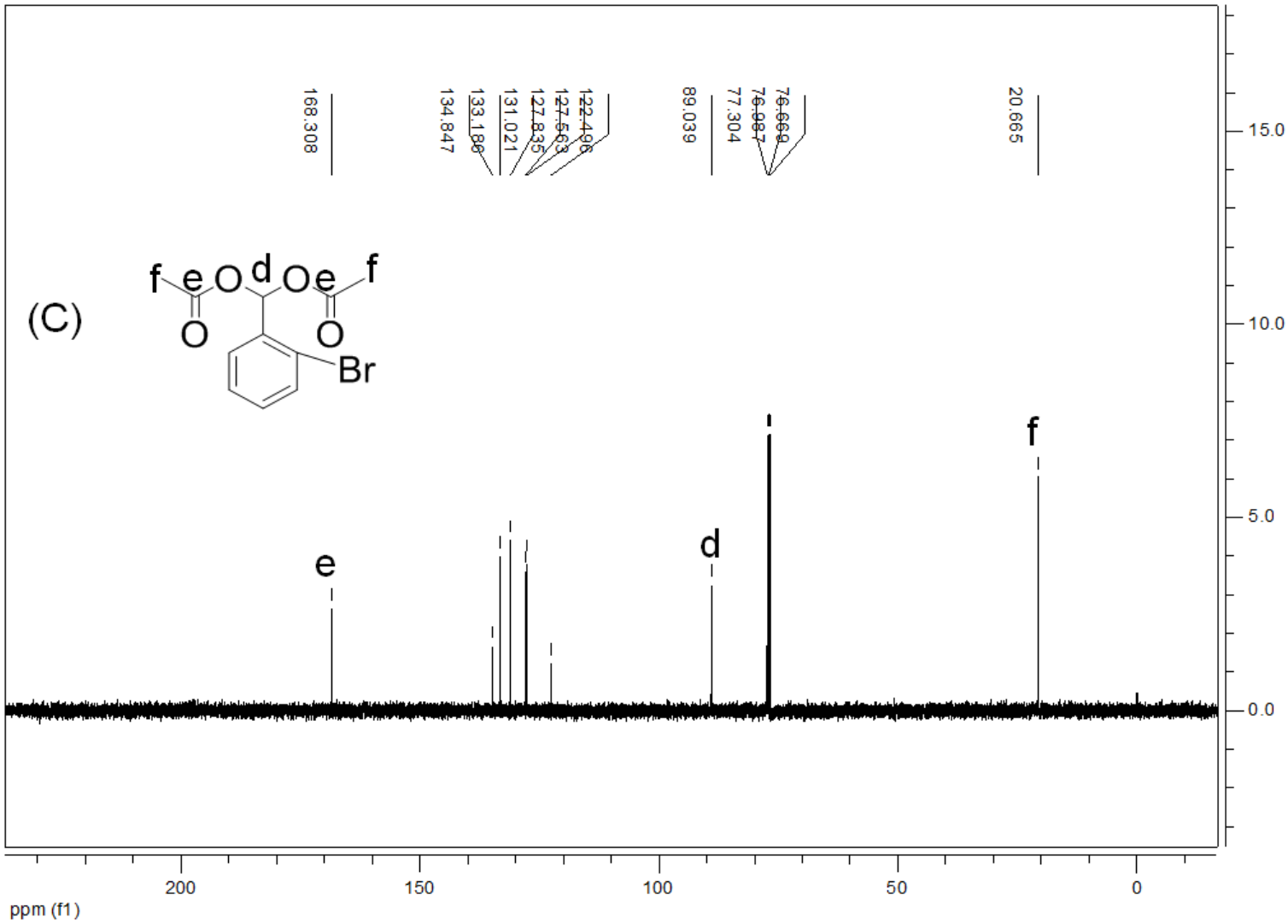

Fig. S15 (C) ^{13}C NMR spectra of entry **11.**

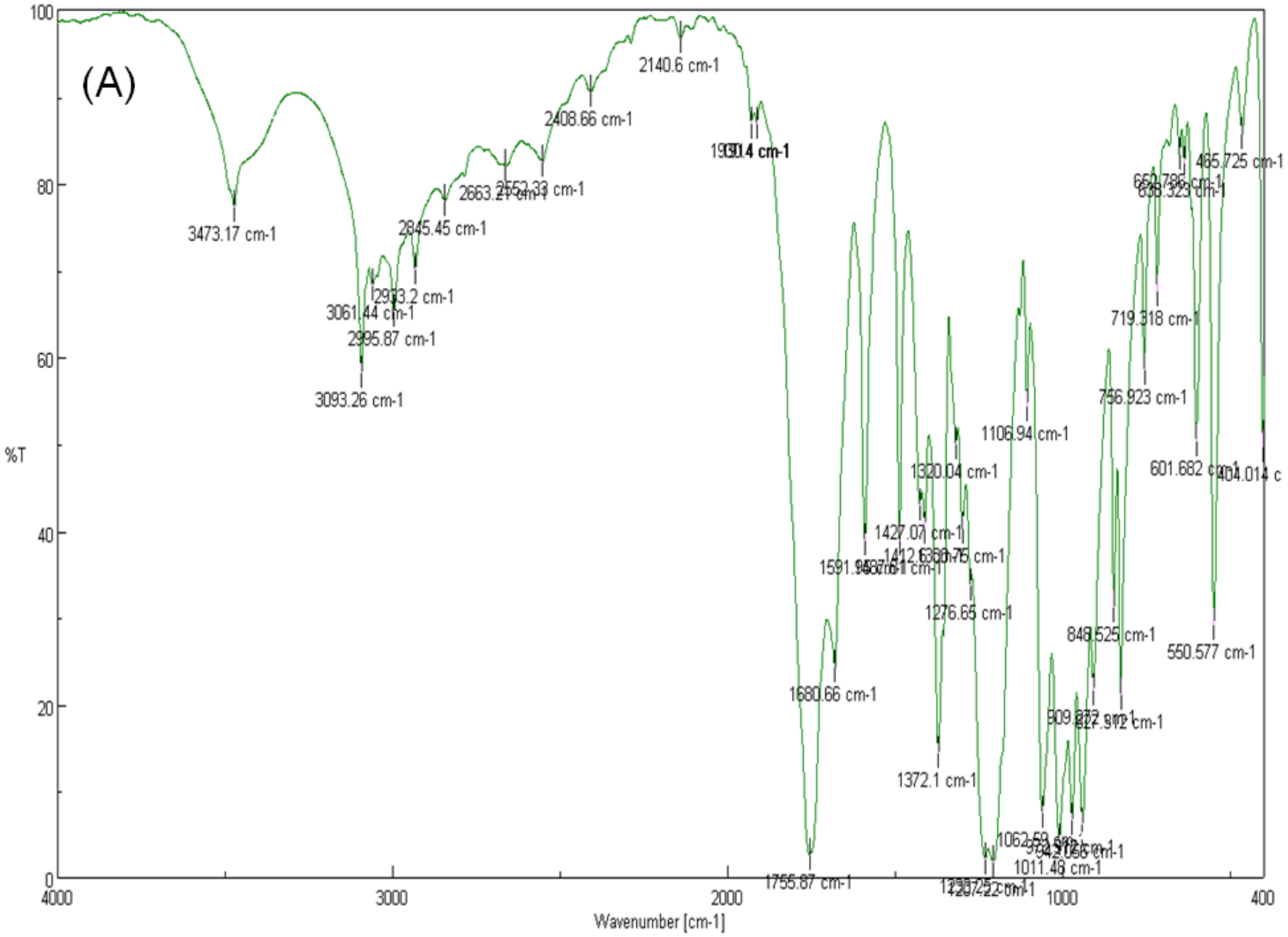

Fig. S16 (A) IR spectra of entry **12.**

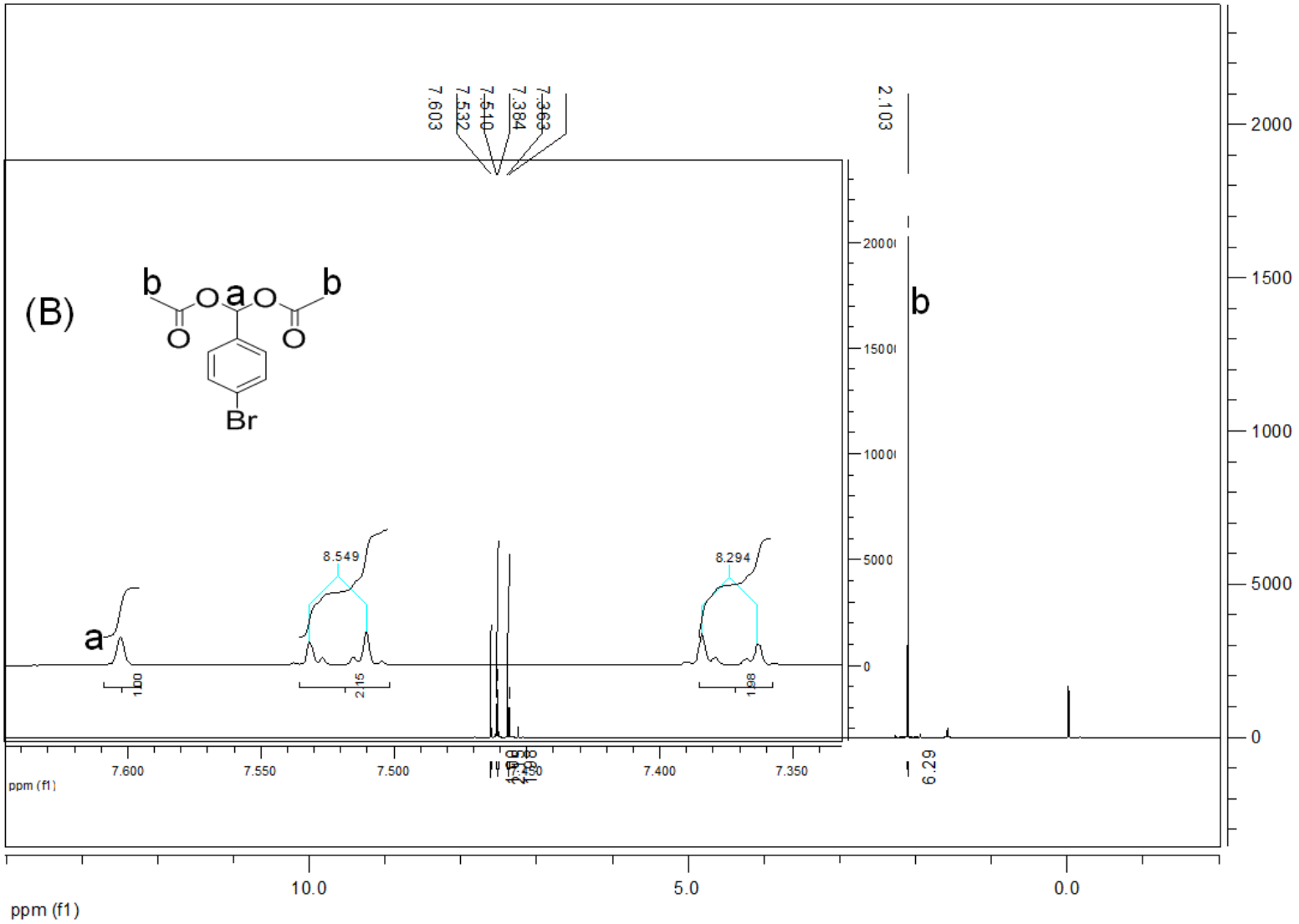

Fig. S16 (B) ^{1}H NMR spectra of entry **12.**

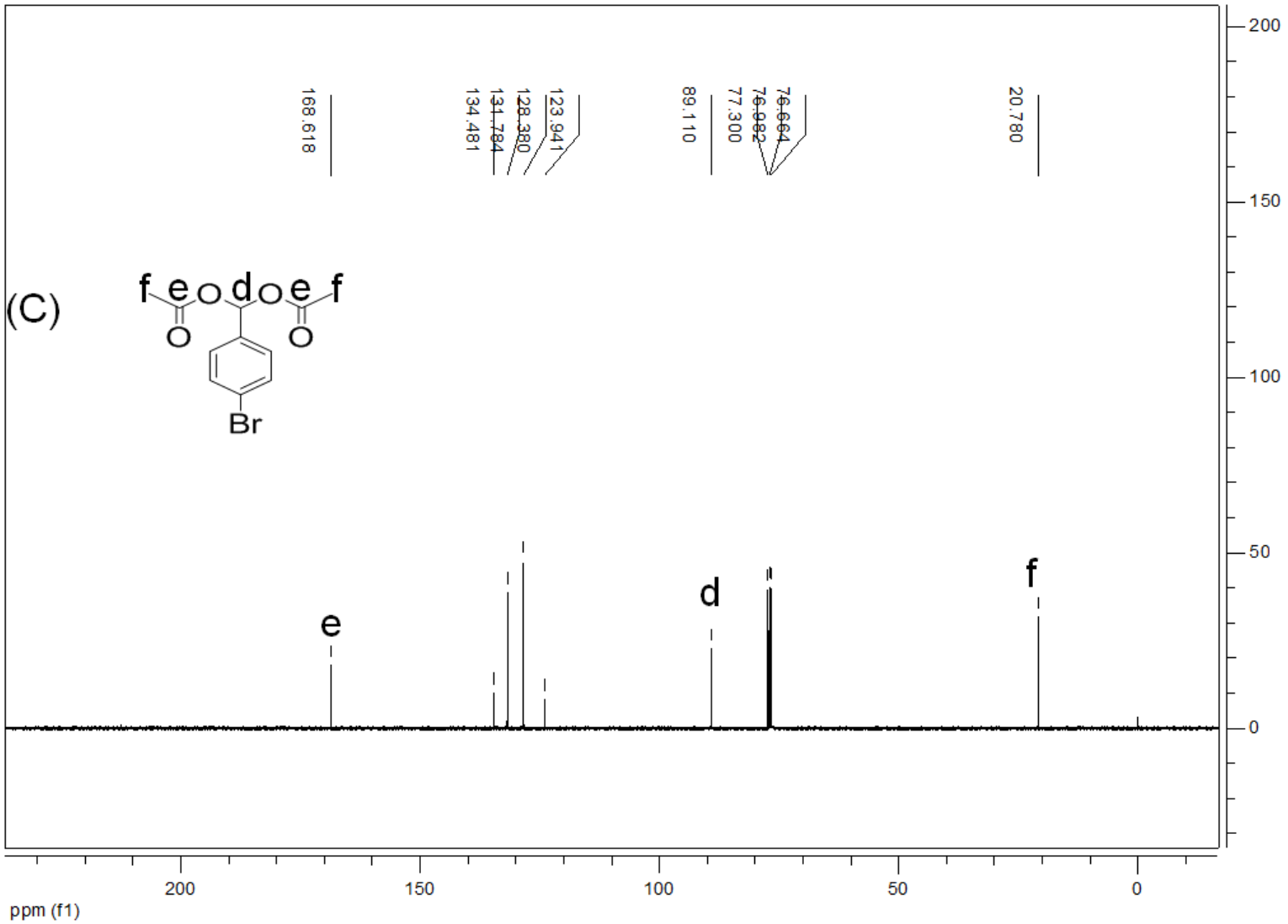

Fig. S16 (C) ^{13}C NMR spectra of entry **12.**

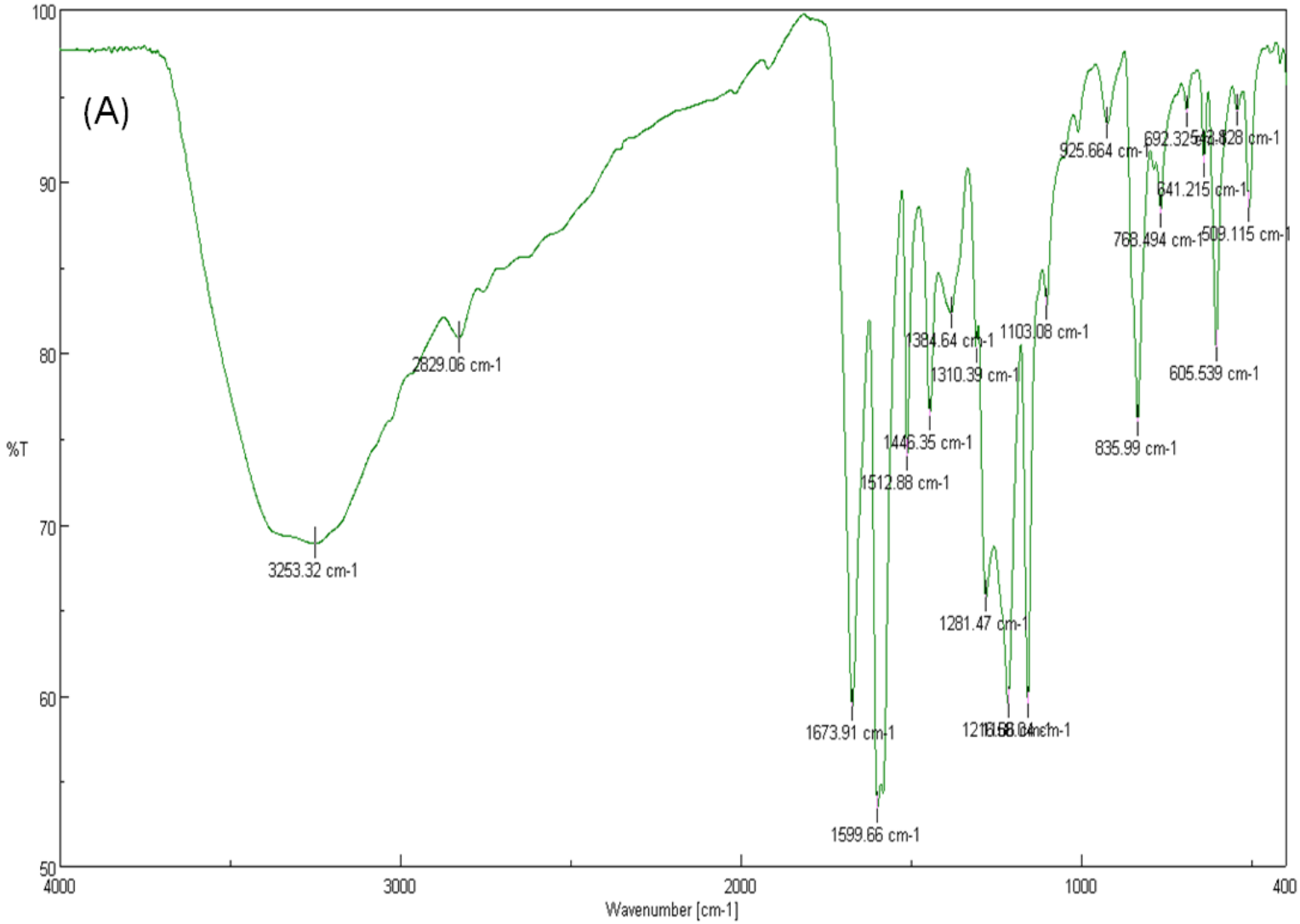

Fig. S17 (A) IR spectra of entry **13.**

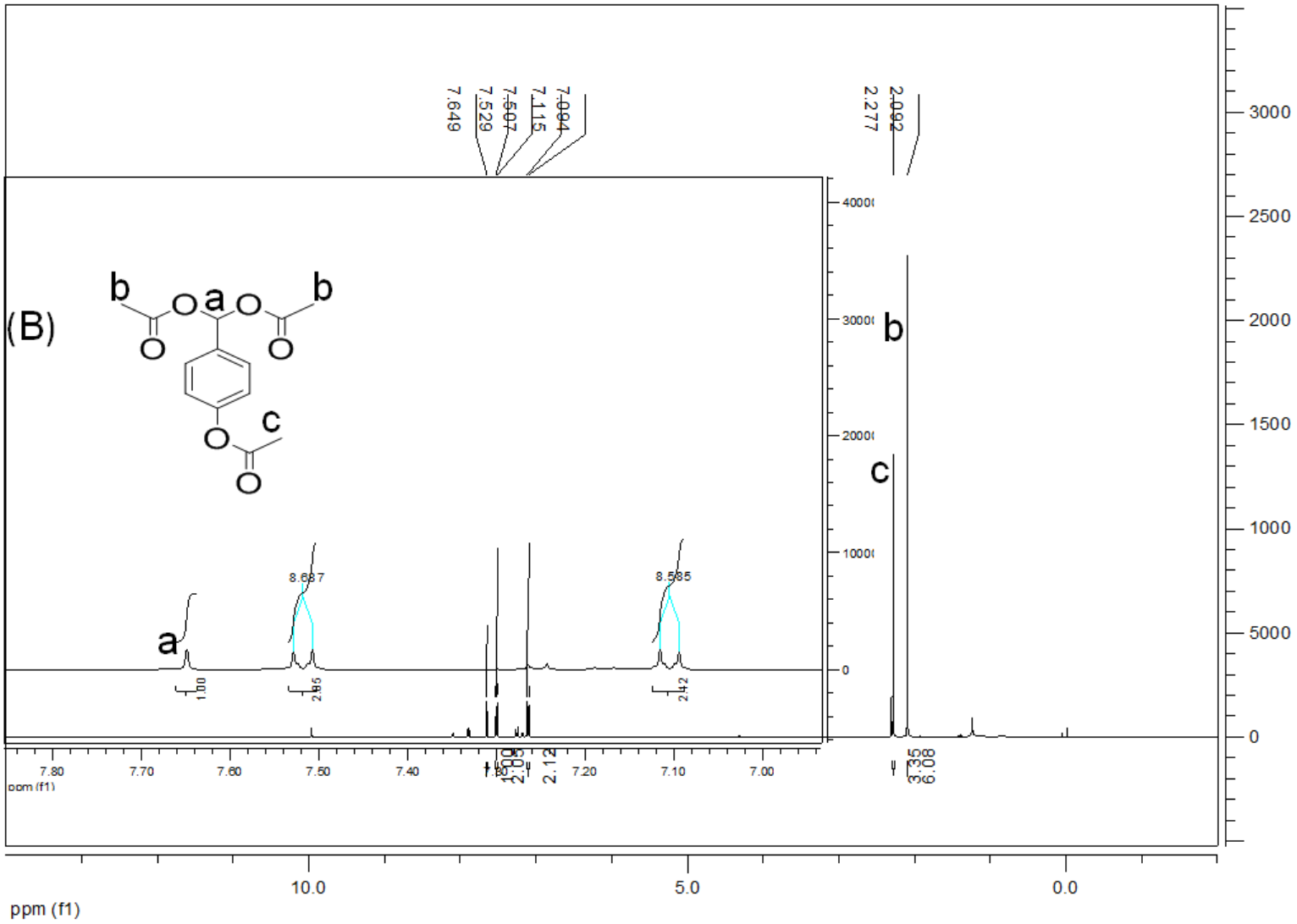

Fig. S17 (B) ^{1}H NMR spectra of entry **13.**

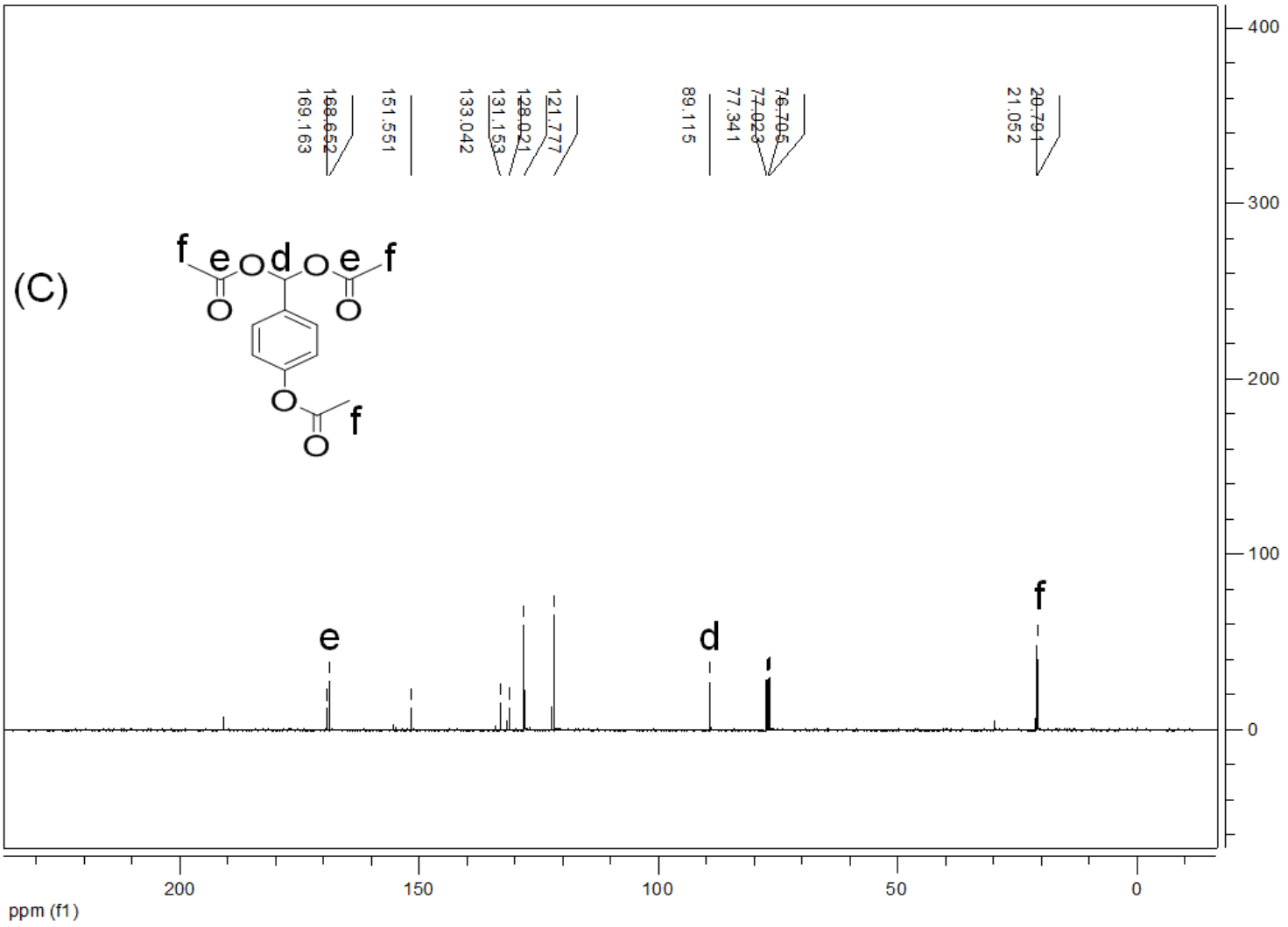

Fig. S17 (C) ^{13}C NMR spectra of entry **13.**

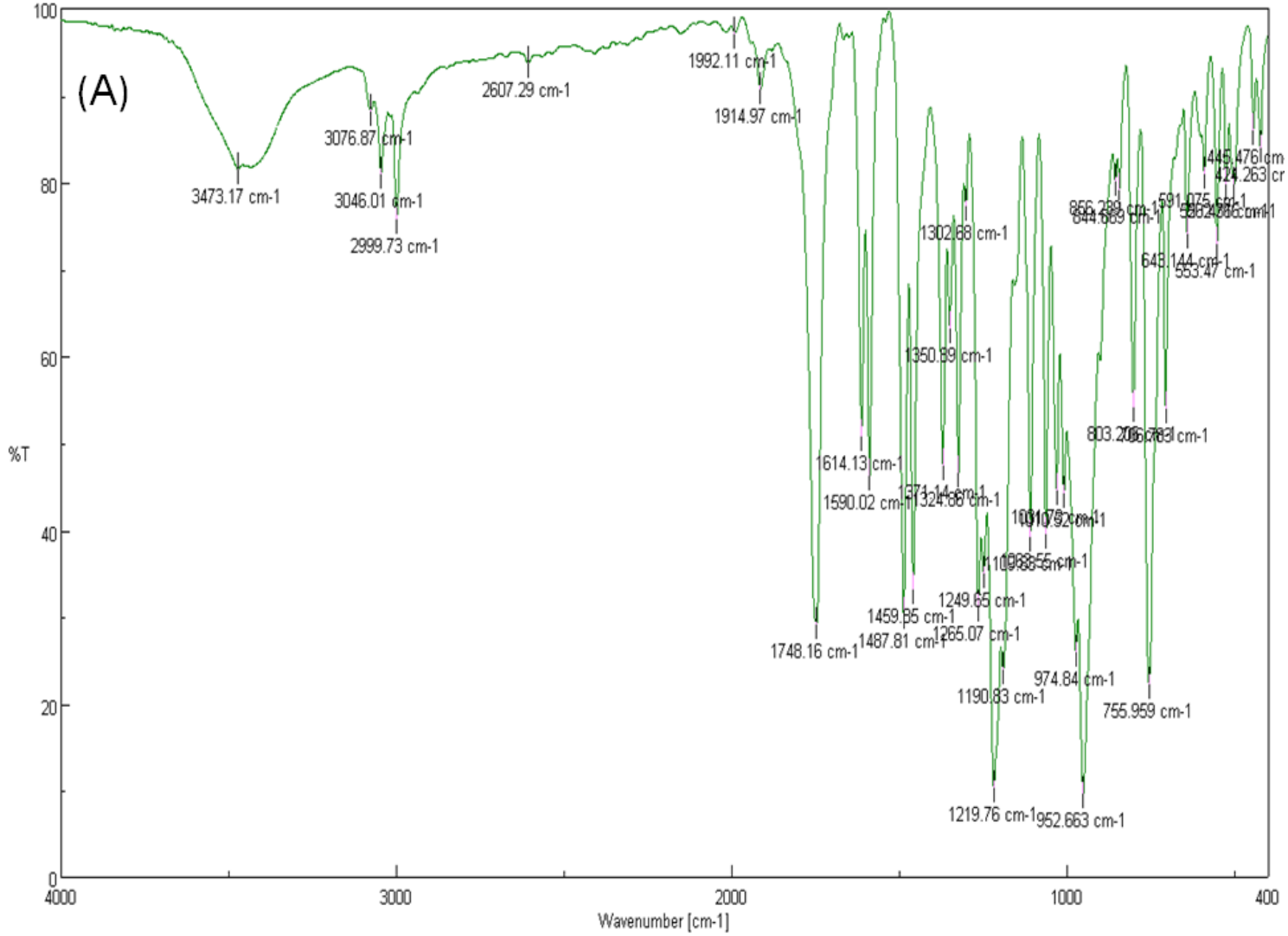

Fig. S18 (A) IR spectra of entry **15.**

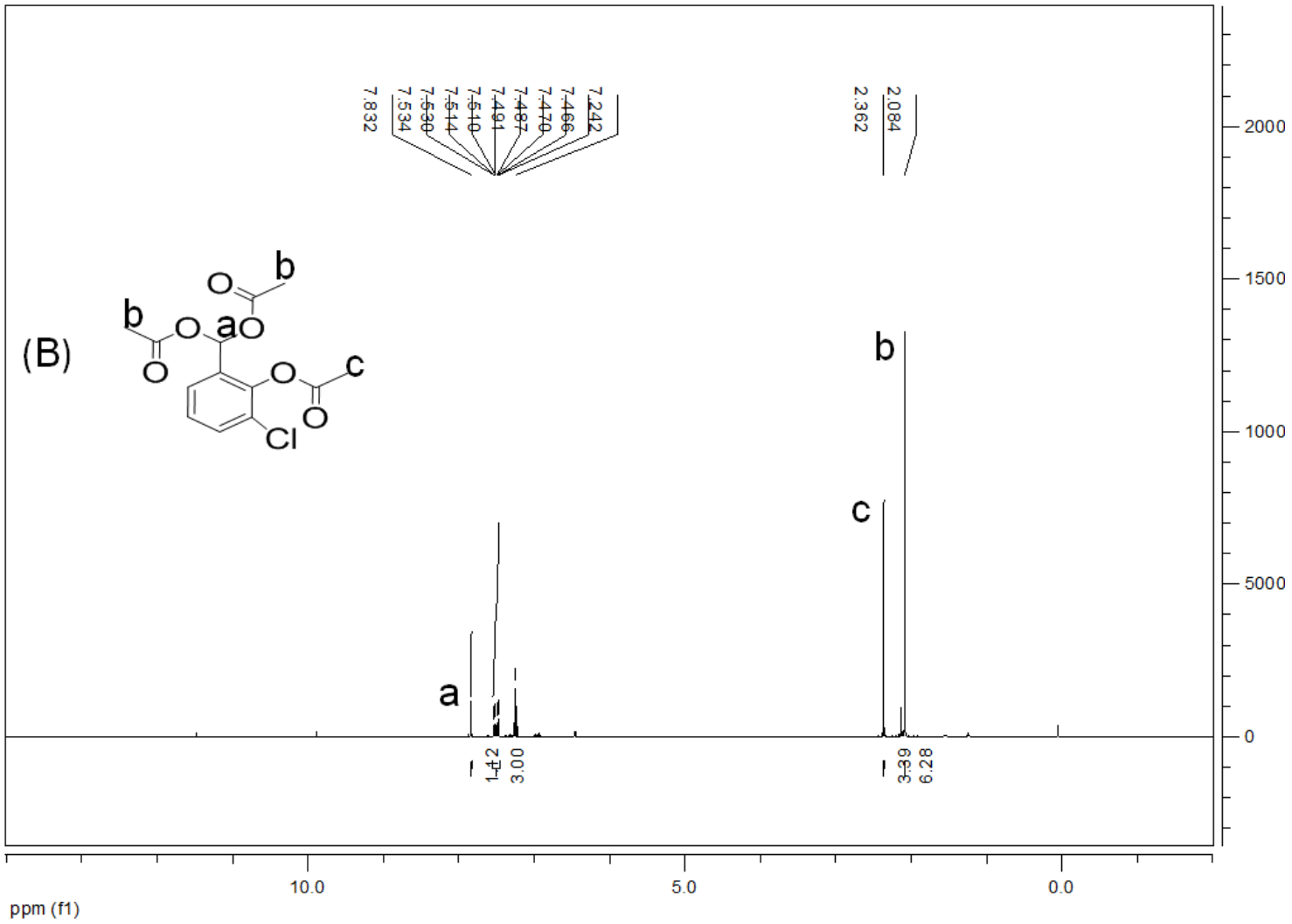

Fig. S18 (B) ^{1}H NMR spectra of entry **15.**

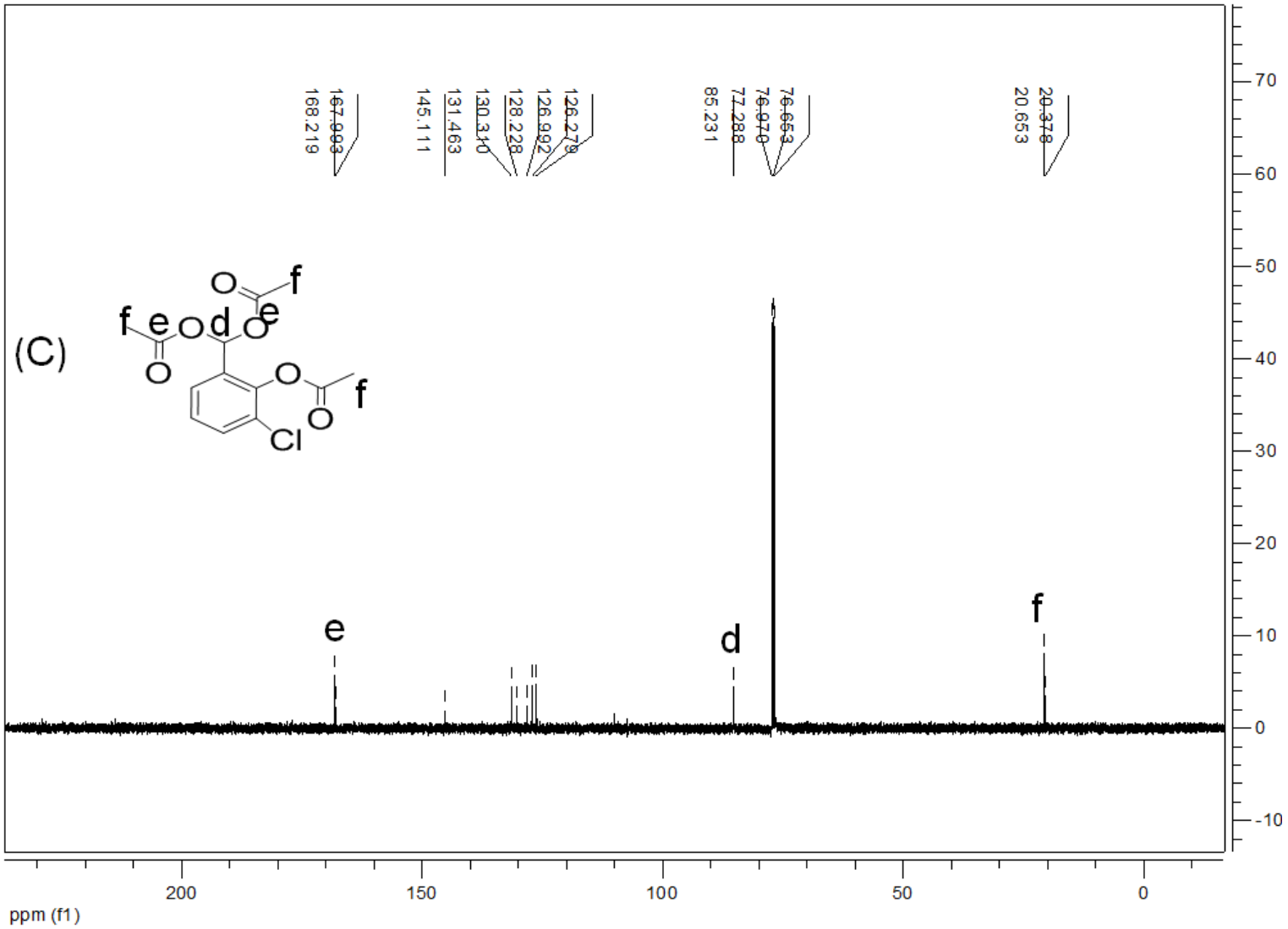

Fig. S18 (C) ^{13}C NMR spectra of entry **15.**

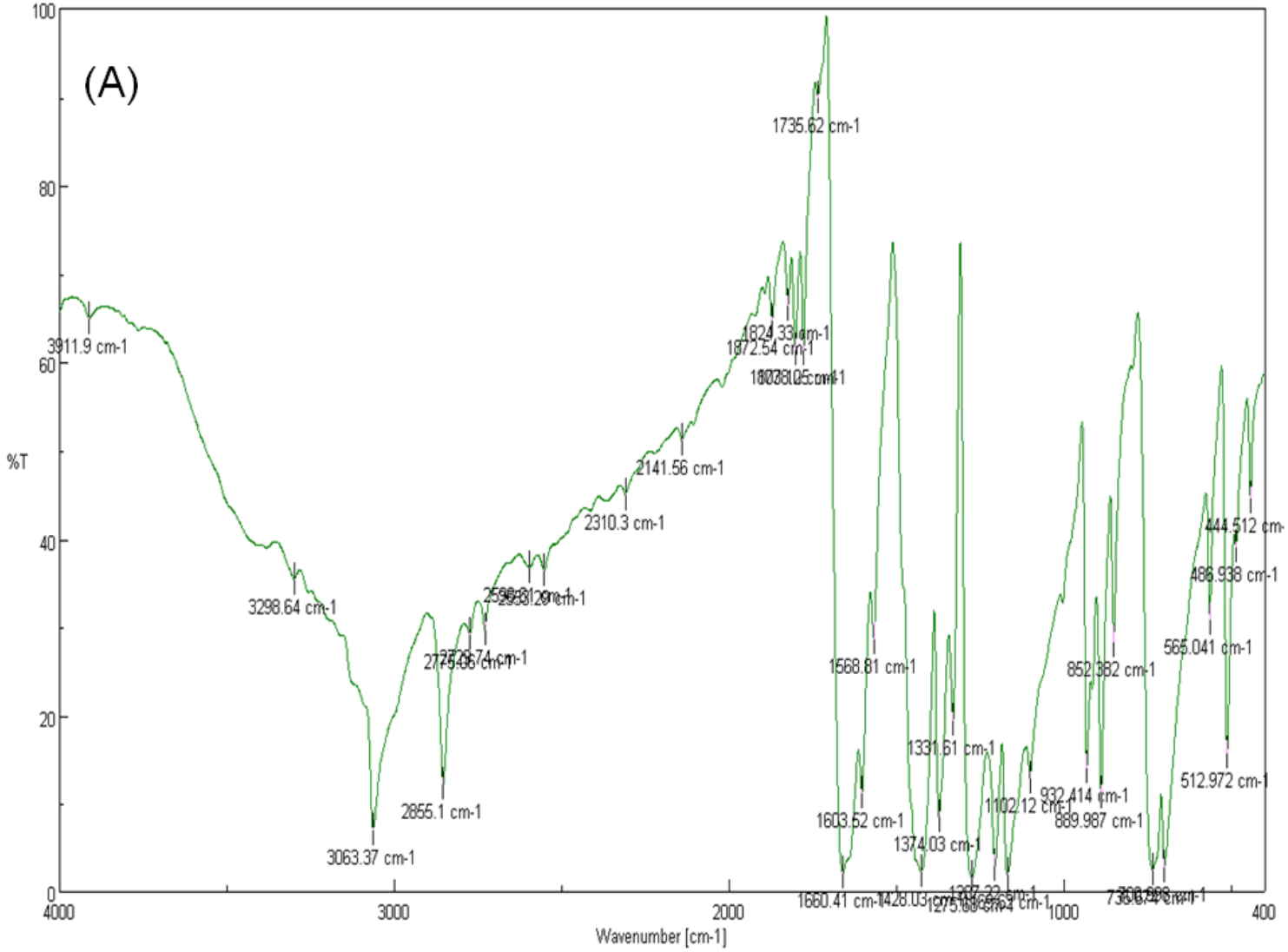

Fig. S19 (A) IR spectra of entry **16.**

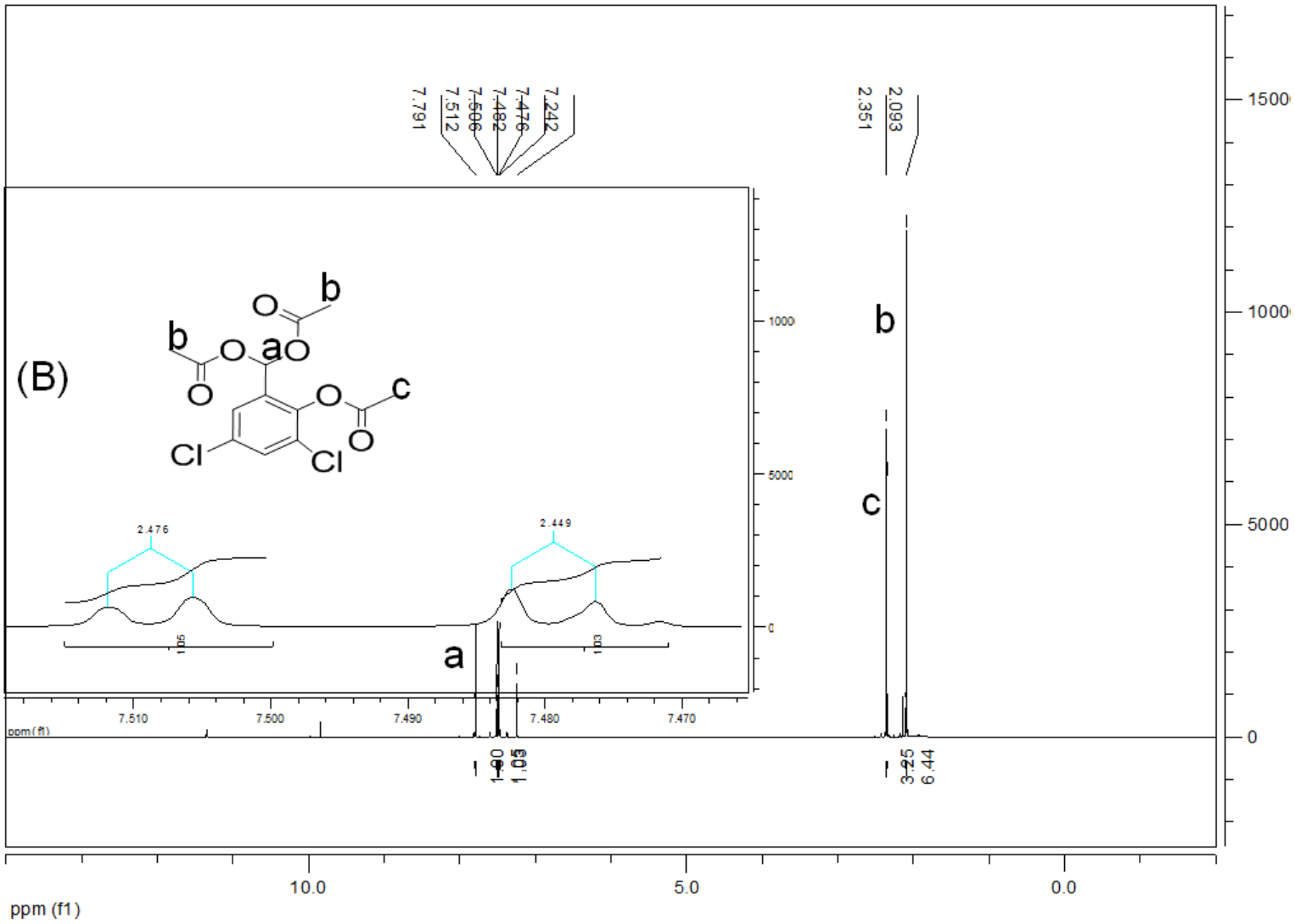

Fig. S19 (B) ^{1}H NMR spectra of entry **16.**

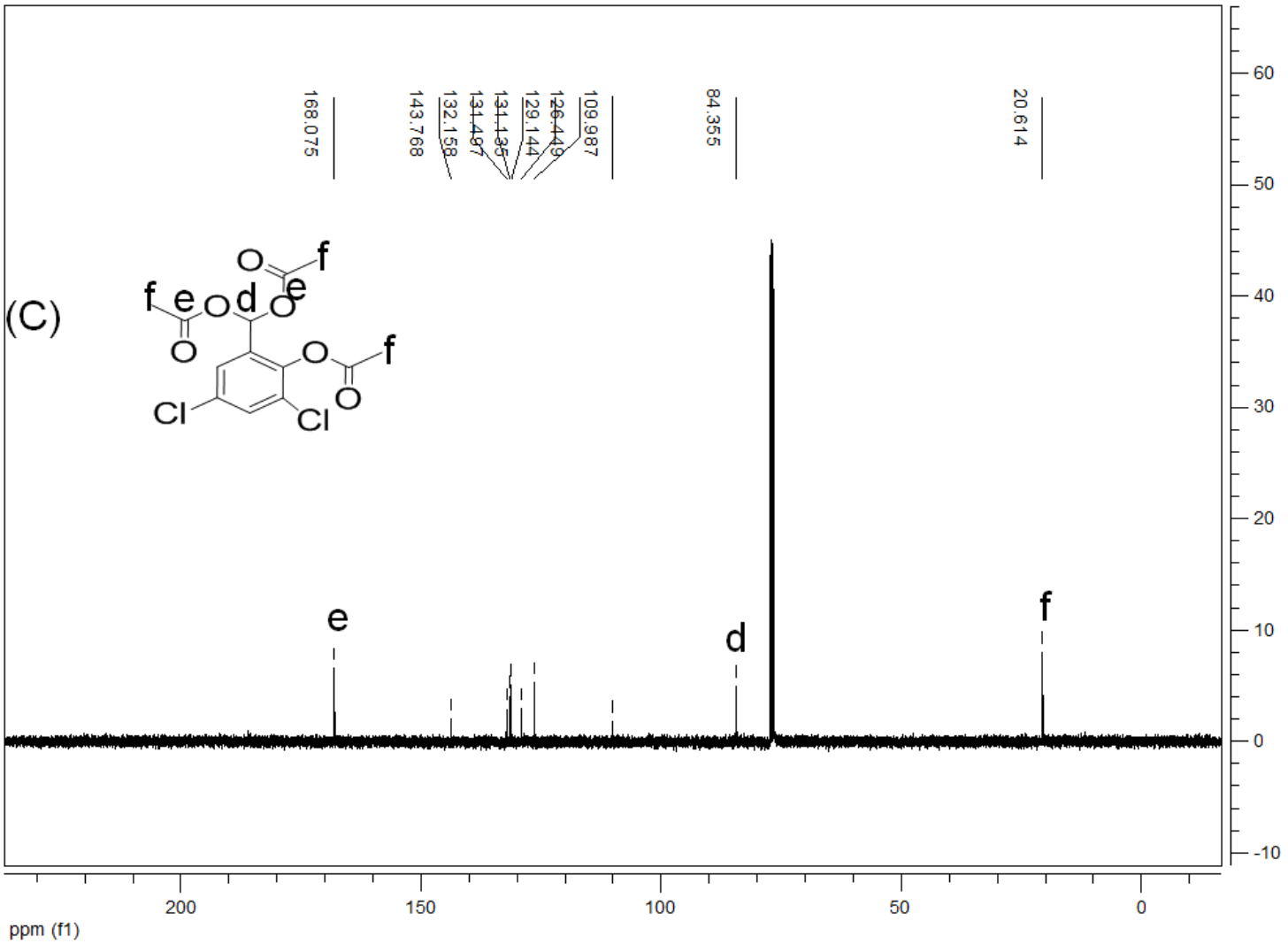

Fig. S19 (C) ^{13}C NMR spectra of entry **16.**

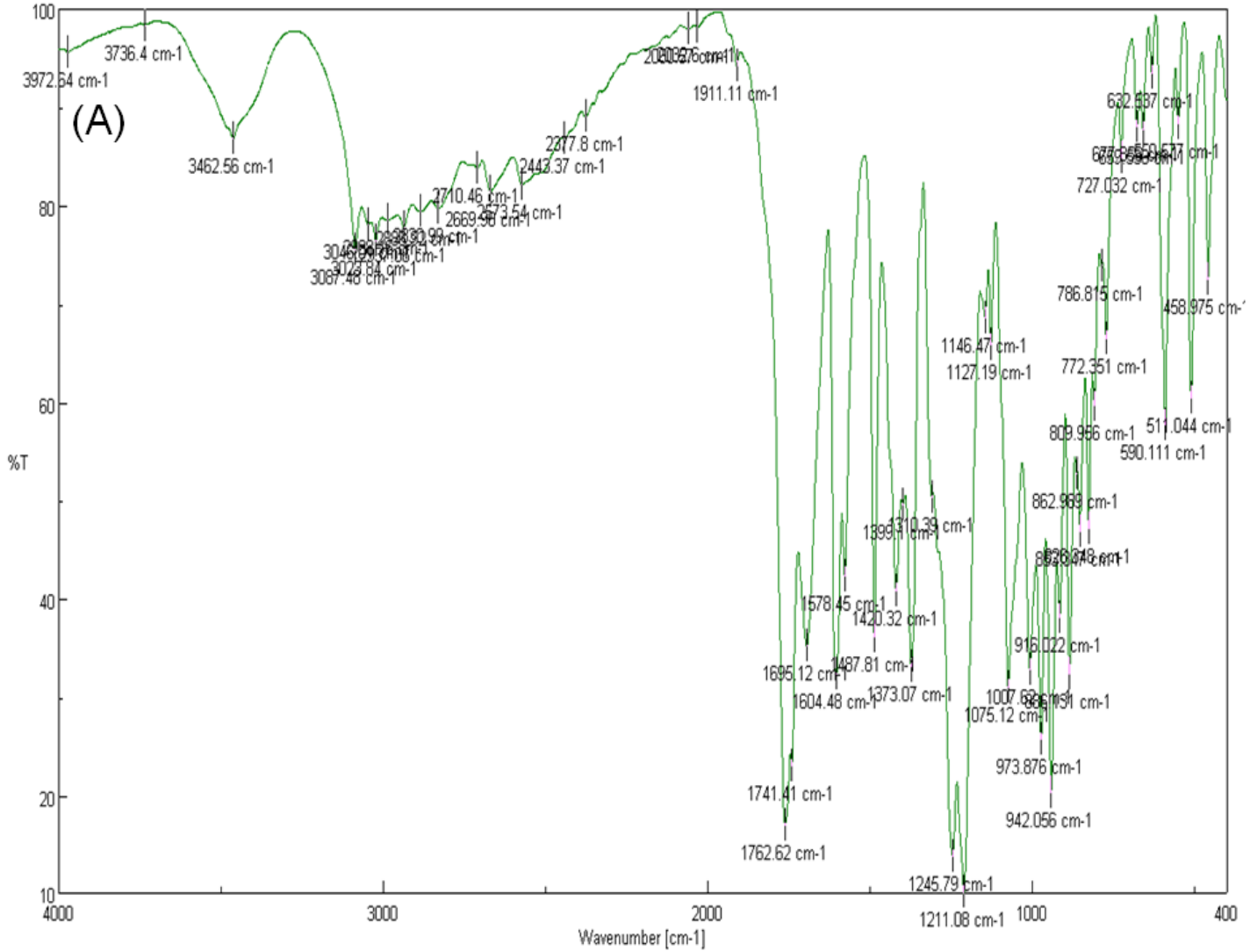

Fig. S20 (A) IR spectra of entry **20.**

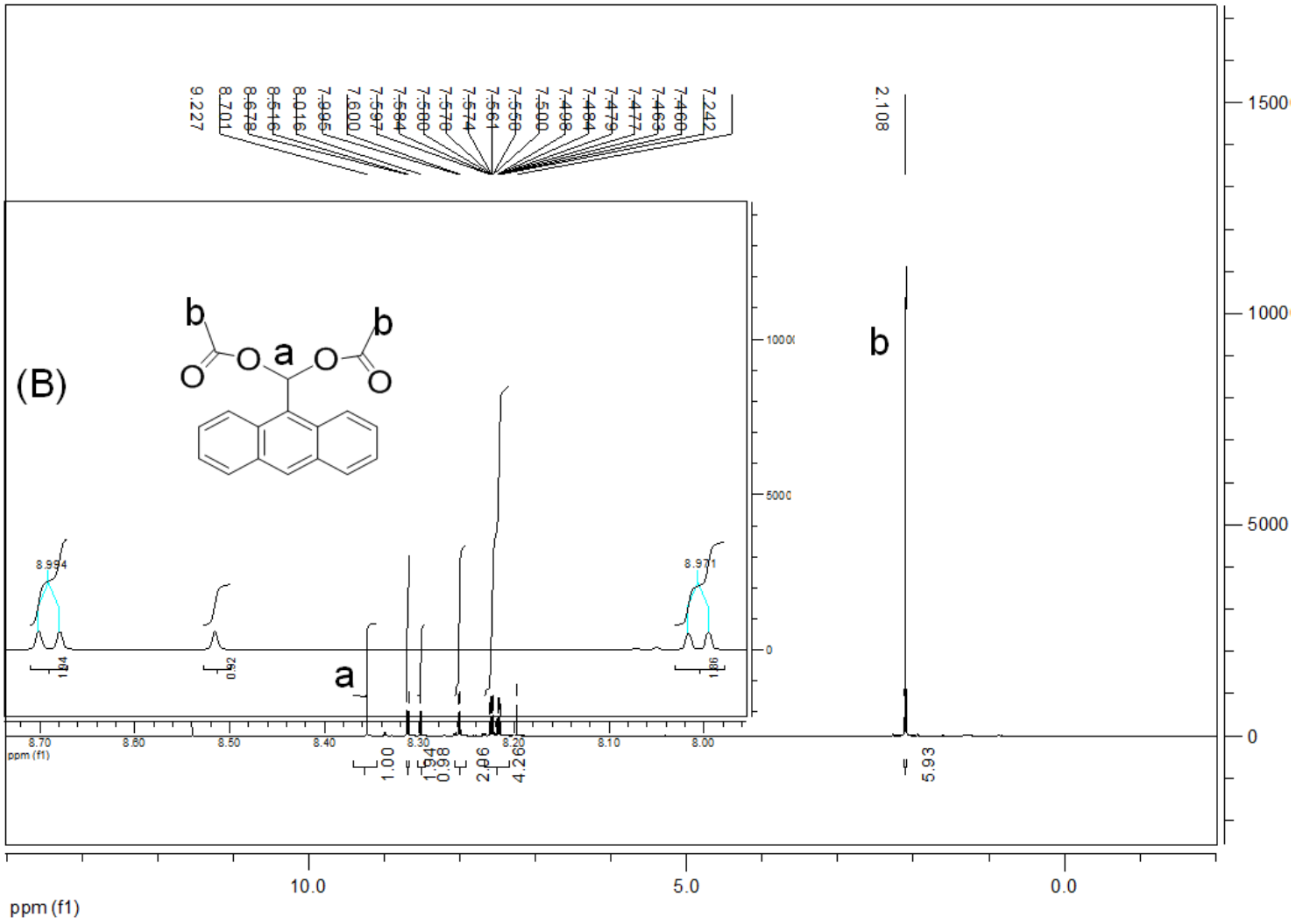

Fig. S20 (B) ^{1}H NMR spectra of entry **20.**

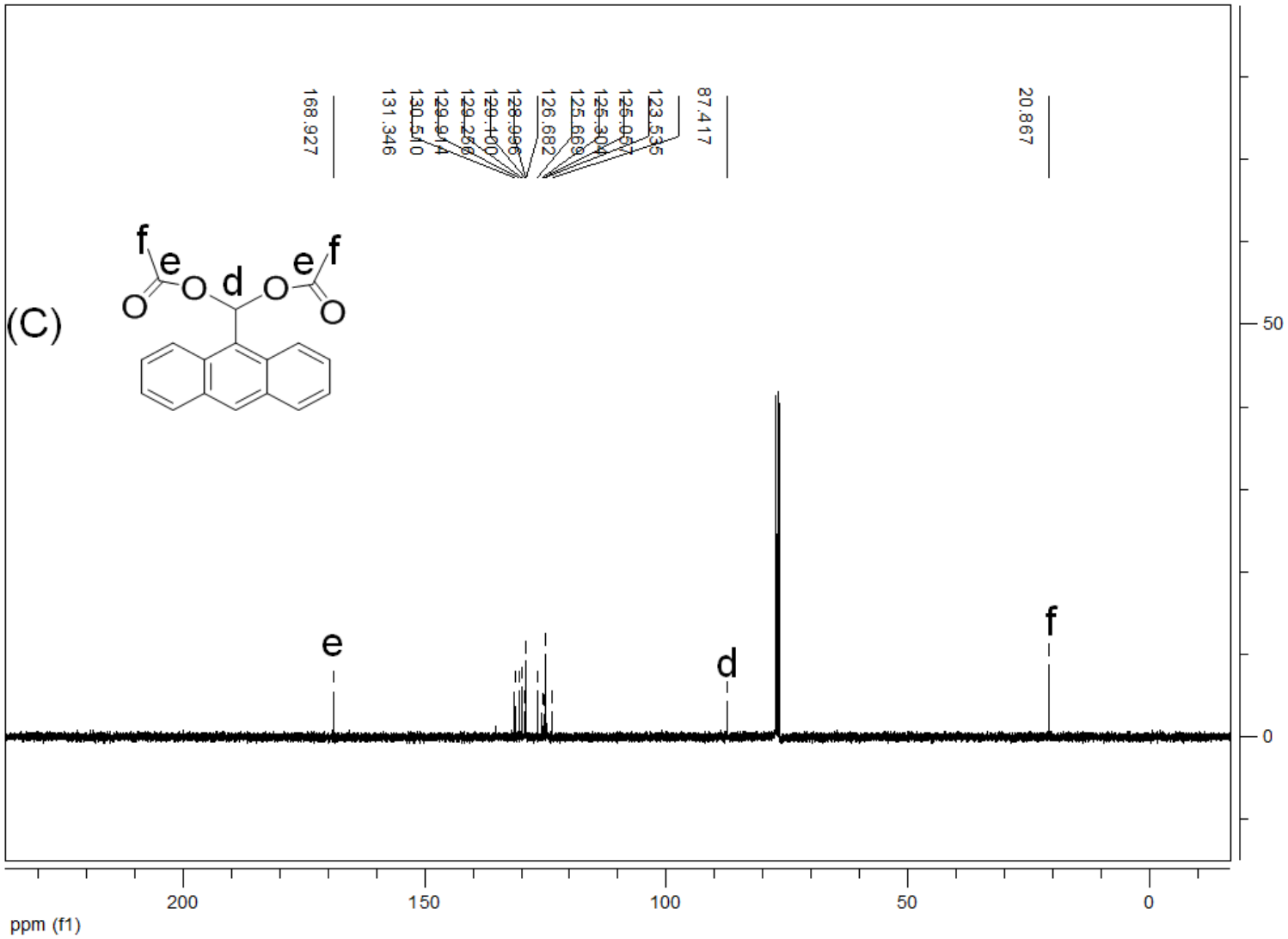

Fig. S20 (C) ^{13}C NMR spectra of entry **20.**

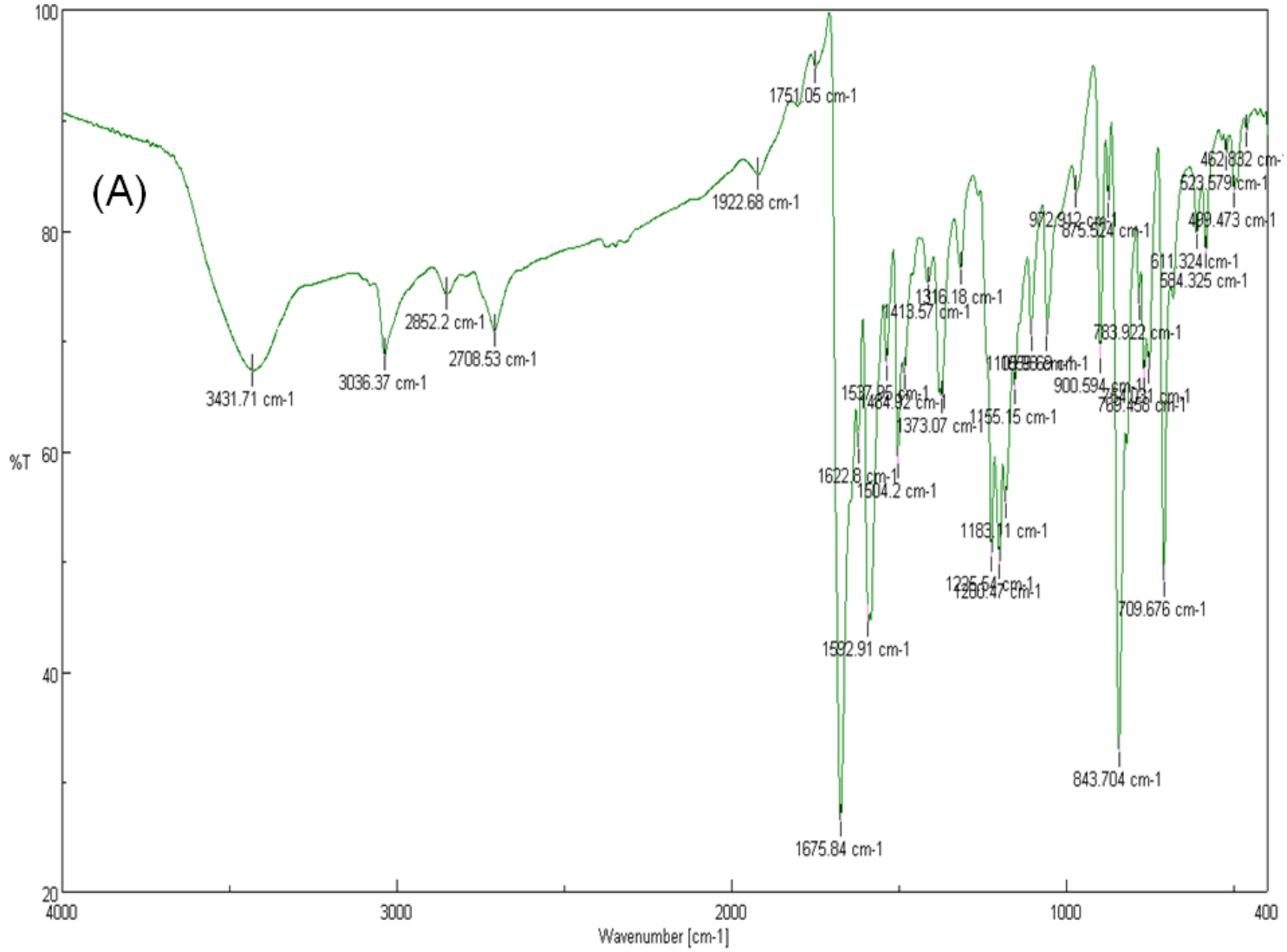

Fig. S21 (A) IR spectra of entry **21.**

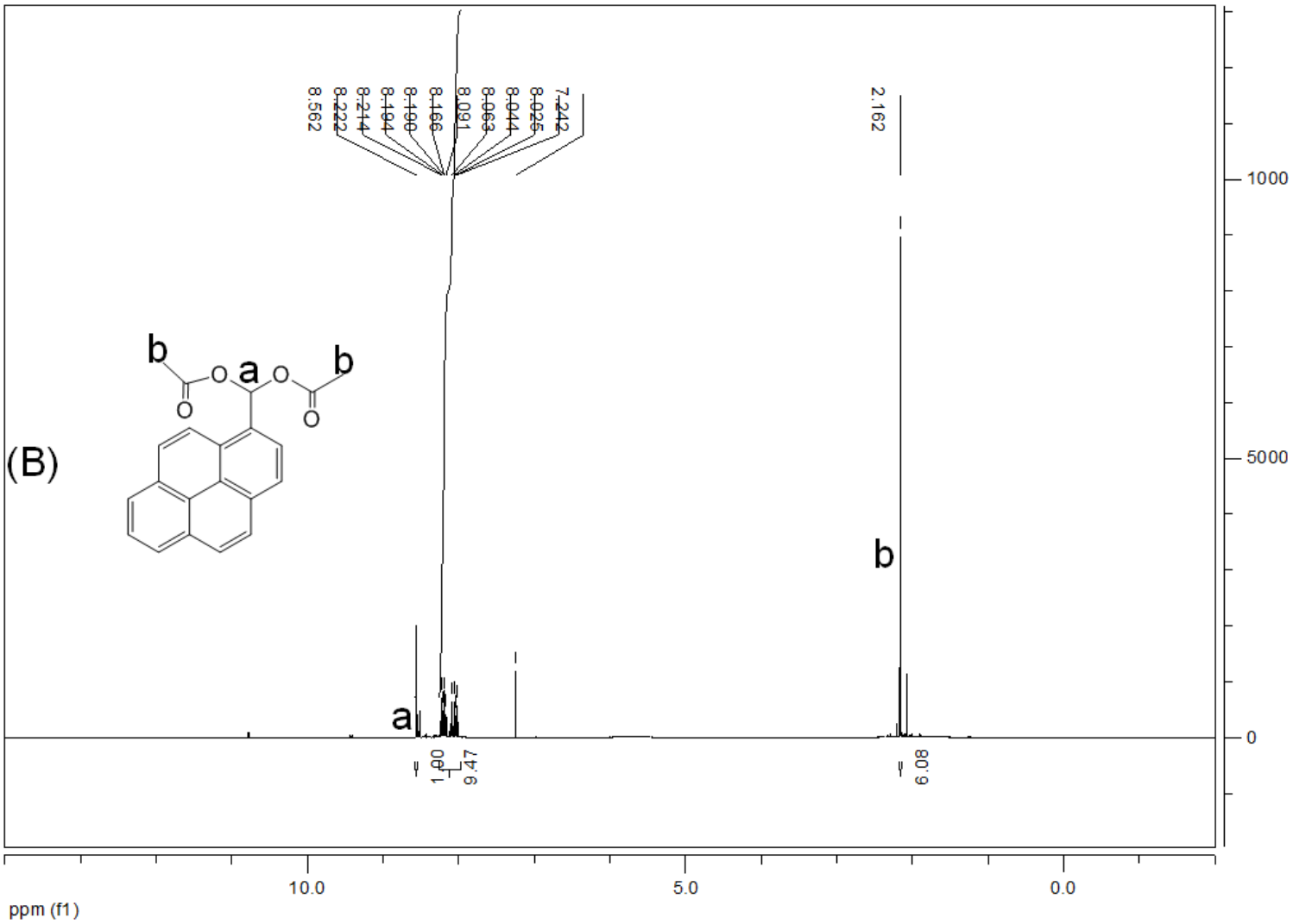

Fig. S21 (B) ^{1}H NMR spectra of entry **21.**

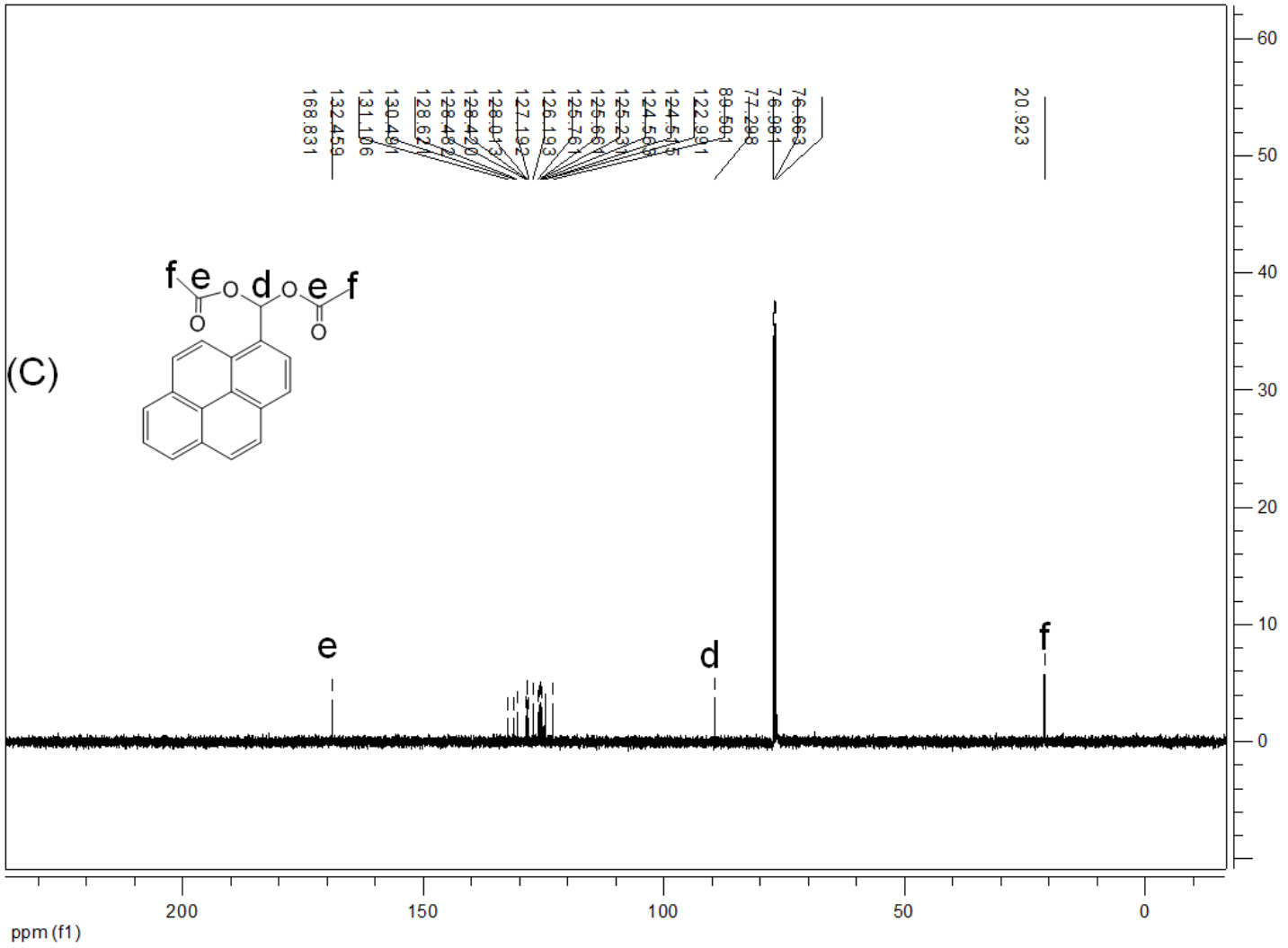

Fig. S21 (C) ^{13}C NMR spectra of entry **21.**

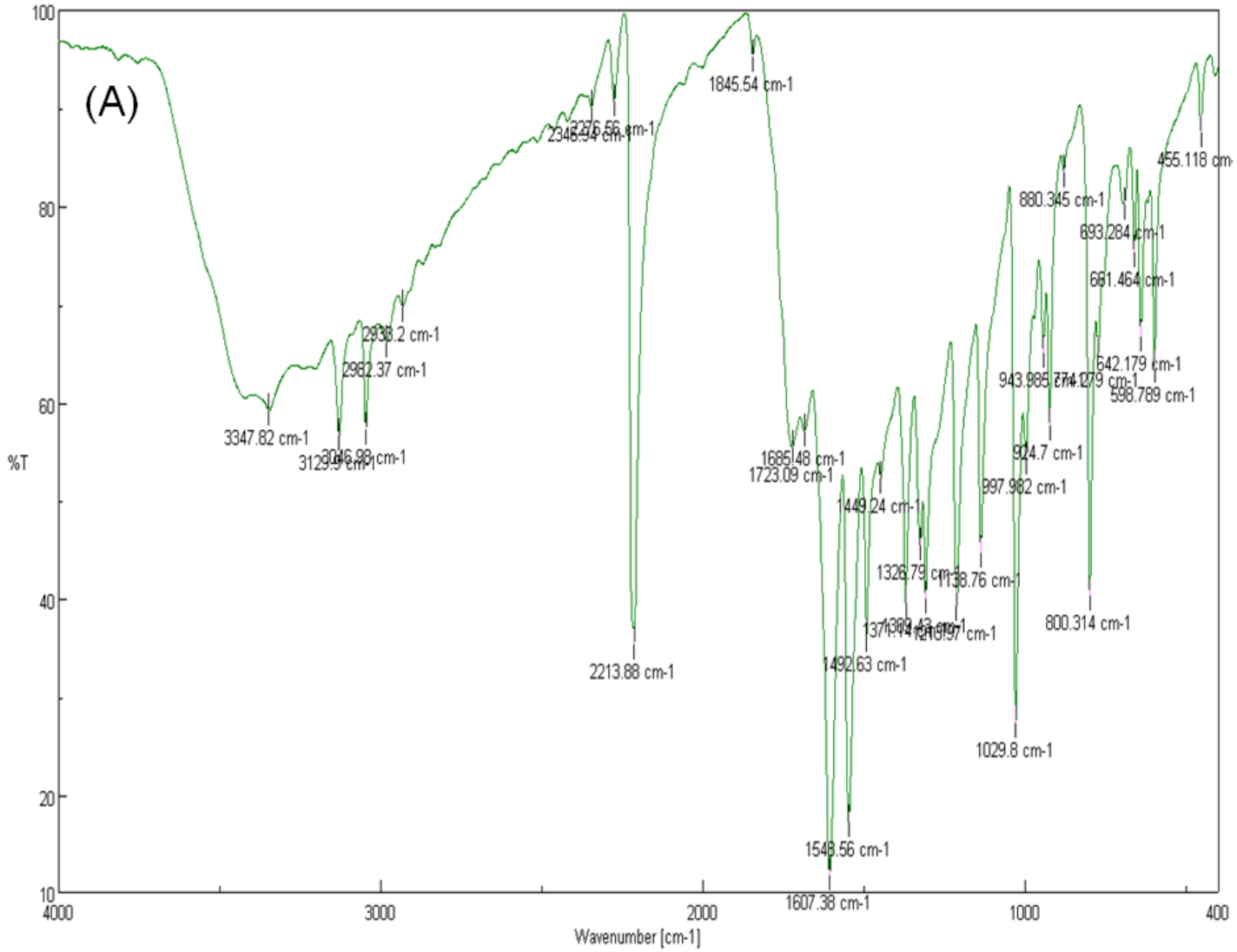

Fig. S22 (A) IR spectra of entry **22.**

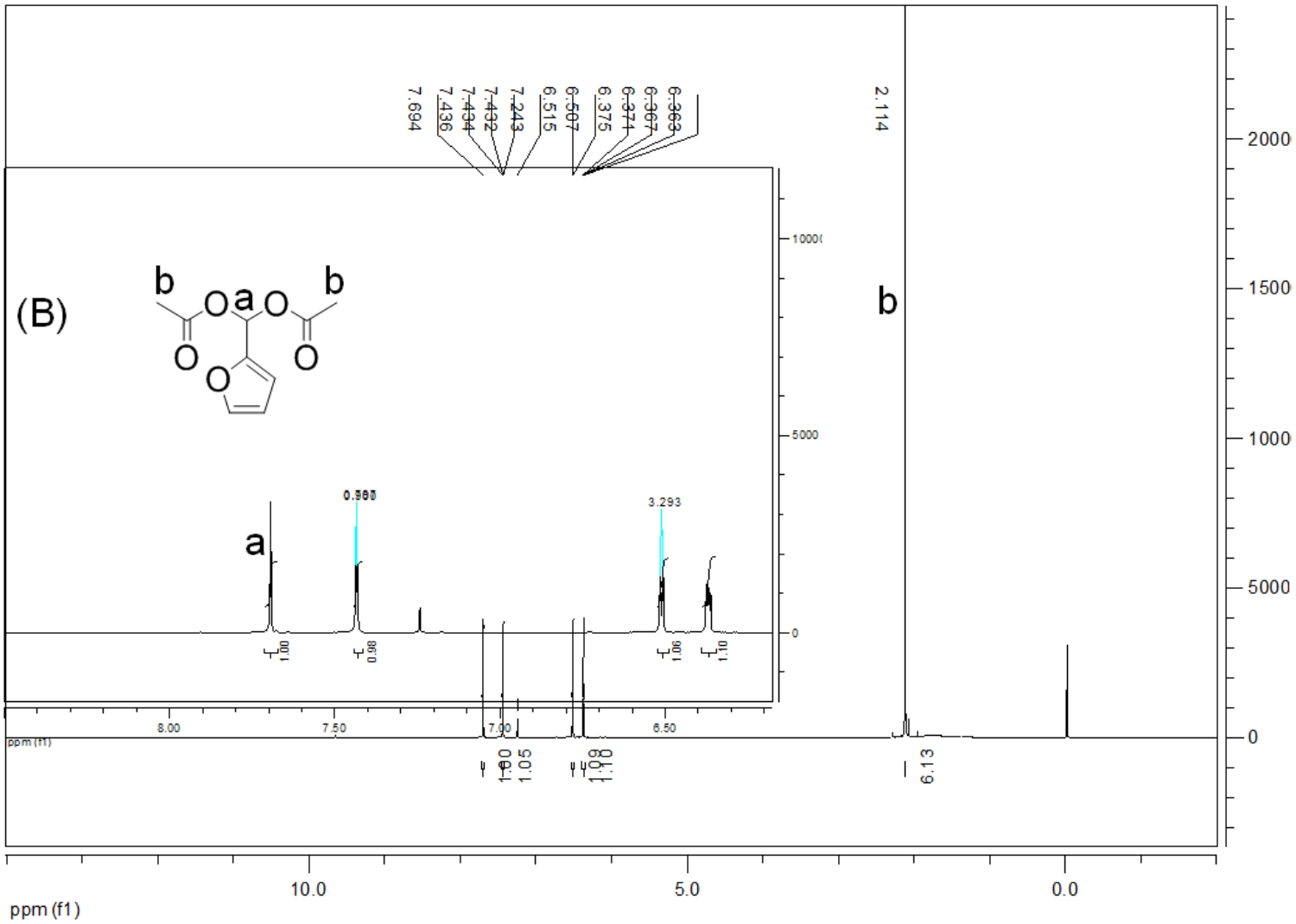

Fig. S22 (B) ^{1}H NMR spectra of entry **22.**

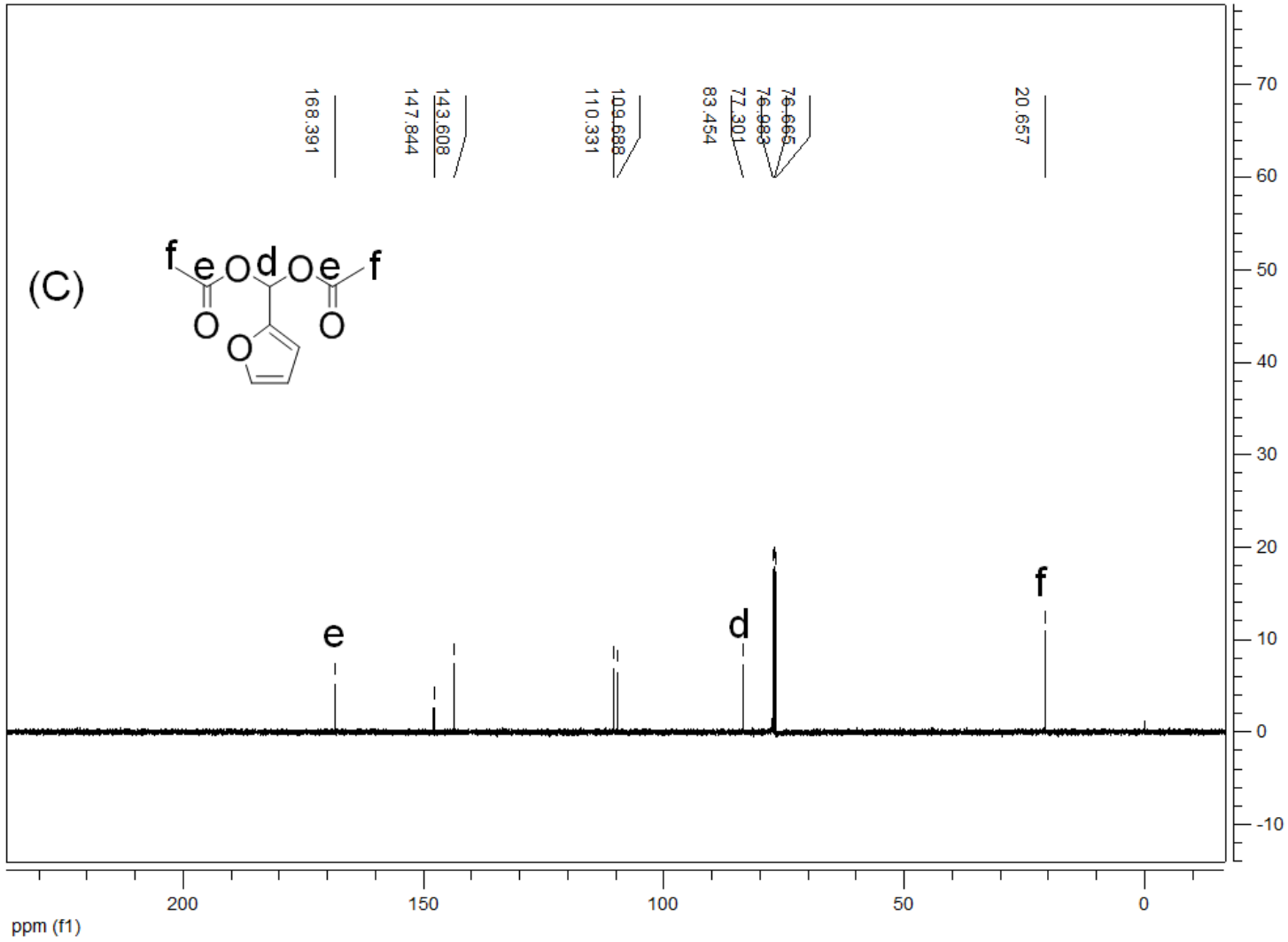

Fig. S22 (C) ^{13}C NMR spectra of entry **22.**